CHAPTER IV
EFFECTS OF PROCESS CONDITION AND SOLVENT SYSTEM ON MORPHOLOGICAL APPEARANCE OF ELECTROSPUN POLYSTYRENE FIBERS

4.1 Abstract

In the present contribution, morphological appearance of as-spun polystyrene (PS) fibers was investigated in term of solution and process parameters, i.e. concentration, viscosity, conductivity, and surface tension of the solutions, emitting electrode polarity, salt addition, applied voltage, and collection distance. Furthermore, the effect of solvent system in either single (i.e. 1,2-dichloroethane (DCE), *N,N*-dimethylformamide (DMF), ethylacetate (EA), and methylethylketone (MEK)) or mixed solvent (i.e. DMF/DCE, DMF/EA, and DMF/MEK) systems was investigated. To observe the effect of the spinning condition, the electrical field strength was varied (i.e. 1:1, 2:1, or 3:1 kV/cm), either by fixing the collection distance (i.e. 7 kV/7cm, 14 kV/7cm, or 21 kV/7 cm) or by fixing the applied voltage (i.e. 25 kV/25 cm, 25 kV/12.5 cm, or 25 kV/8.3 cm). In all of the spinning conditions investigated, the collection time was fixed at about 15 seconds. The morphological appearance of the fibers was investigated by scanning electron microscopy (SEM).

KEYWORDS: Electrospinning/ Polystyrene/ Ultrafine Fiber

4.2 Introduction

When the diameter of a polymeric fiber decreases from micrometers down to sub-micrometers or even nanometers, there appear to be several amazing characteristics such as high surface area to volume ratio, flexibility in surface functionalities, and improved mechanical properties. These outstanding properties make polymeric electrospun nanofibers as excellent candidates for many important applications, some of which are filtration, reinforcing materials, wound dressing, tissue scaffolding, controlled release materials, and so on so forth [1].

The electrospinning process seems to be the only method which can be further developed for mass production of continuous nanofibers from various polymers, without the need of a special technique. Some advantages of the process are simple tooling, cost-effectiveness, and ability for producing highly-oriented fibrous mats with small pore sizes between depositing fibers. Consequently, the process has entertained much interest from scientists and technologists alike, thanks partly to the world-wide interest on nanoscience and nanotechnology.

Set-up of the electrospinning process is very simple. The three major components are a high-voltage power supply, a container of a polymer solution or melt with a small opening, and a conductive collective screen. The emitting electrode of the power supply is connected to the polymer solution or melt, while the grounding one is connected to the screen collector to complete the electrical circuit. Mutual charge repulsion generated within the polymer solution or melt destabilizes the normally hemispherical pendant drop at the tip of a nozzle connected to the small opening of the container into a conical shape, called the Taylor's cone at a critical value of the electrostatic field strength. Further increasing the electrostatic field strength causes an electrically-charged stream (i.e. jet) of polymer solution or melts to be ejected from the cone's apex as a means of reducing the accumulating surface charges. The jet travels in a straight trajectory for only a short distance before undergoing a bending instability that causes the conical looping trajectory with the apex locating at the onset point of the bending instability. Finally, the jet rests on the collective screen as dried or solidified fibers [2].

In the electrospinning process of a polymer solution, a number of parameters affect the morphology of the obtained fibers. These governing parameters are (i) solution (e.g. concentration, viscosity, conductivity, and surface tension of the polymer solutions), (ii) process (e.g. applied voltage, collection distance, emitting electrode polarity, and feed rate), and (iii) ambient (e.g. temperature, relative humidity, and velocity of the surrounding air in the spinning chamber) parameters [3]. Formhals [4] was the first to file the patent on such processes, while Baumgarten [5] was the first to systematically study the application of the processes as a means to produce fibers, using polyacrylic as the model system. He found that an increase in the solution viscosity was responsible for the observed increase in the average fiber diameter, while an increase in the flow rate of the solution did not affect significantly the diameters of the resulting fibers.

Fong *et al.* [6] investigated the formation of minute beads on the as-spun poly(ethylene oxide) (PEO) fibers by relating the phenomenon to the properties of the solutions. They found that the number of beads decreased with increasing viscosity, net charge density and decreasing surface tension coefficient of the solutions. Choice of solvent or a combination of solvents used was also found to have a significant effect on the morphology of the as-spun fibers. Lee *et al.* [7] reported the formation of as-spun poly(ε-caprolactone) (PCL) from PCL solutions in a mixture of methylene chloride and *N,N*-dimethylformamide (DMF). They found that spinnability and diameters of the obtained fibers dramatically decreased with increasing DMF content, due possibly to the increased conductivity of the resulting solutions.

Actual utilization of electrospun fibers in the industries is hampered by the extremely low electrospinnability of the process. Very recently, Jarusuwannapoom *et al.* [8] reported that choice of the solvent used to prepare polystyrene (PS) solutions had a profound effect on the electrospinnability of the resulting solutions. Among the eighteen solvents investigated, they reported that PS solutions in 1,2-dichloroethane (DCE), DMF, ethylacetate (EA), methylethylketone (MEK), and tetrahydrofuran (THF) could produce electrospun PS fibers with high enough electrospinnability, while the PS solutions in benzene, cyclohexane, decalin, ethylbenzene, nitrobenzene, and tetralin were not spinnable. Qualitative observation

of the results obtained suggest that the important factors determining the electrospinnability of the as-prepared PS solutions are high enough values of both the dipole moment of the solvent and the conductivity of both the solvent and the resulting solutions, high enough boiling point of the solvent, not-so-high values of both the viscosity and the surface tension of the resulting solutions.

The main objective of this work was to systematically study the electrospinning of PS solutions in single or mixed solvent systems of DCE, DMF, EA, and MEK against some of the solution (i.e. concentration, viscosity, conductivity, and surface tension of the solutions) and the process parameters (i.e. applied voltage, collection distance, and emitting electrode polarity). The morphological and size of the as-spun fibers were characterized mainly by scanning electron microscopy (SEM). Furthermore, the effect of inorganic salt addition on morphological and size of the as-spun fibers was also investigated.

4.3 Experimental

4.3.1 Materials

The polystyrene (PS) resin ($M_w \approx 3.0\times10^5$ Daltons and polydispersity = 2.51) was a general purpose grade (685D, Dow Plastic, USA). The four solvents used in this work were 1,2-dichloroethane [DCE; Labscan (Asia), Thailand], *N,N*-dimethylformamide [DMF; Labscan (Asia), Thailand], ethylacetate [EA; Labscan (Asia), Thailand], and methylethylketone [MEK; Carlo Erba, Italy]. Some important properties of these solvents are summarized in Table 4.1. Lithium chloride [LiCl; Ajax Chemicals, Australia], and potassium chloride [KCl; Ajax Chemicals, Australia] were used as inorganic salts.

4.3.2 Preparation of Spinning Solutions

The spinning solutions were prepared in either single or mixed solvent systems. In either case, a measured amount of PS pellets was dissolved in a measured quantity of DCE, DMF, EA, or MEK for the single solvent system and DMF/DCE, DMF/EA or DMF/MEK in various volumetric ratios of 75/25, 50/50, and 25/75, respectively, for the mixed solvent system to produce PS solutions with

concentrations being 10, 20, or 30% (w/v). Some of the solution properties, i.e. viscosity, conductivity, and surface tension were measured by a Brookfield DV-III programmable viscometer, an Orion 160 conductivity meter, and a Krüss DSA10 Mk2 drop shape analyzer, respectively. To investigate the effect of salt addition, about 1% (w/v) of LiCl or KCl salt was dissolved in the as-prepared PS solutions.

4.3.3 Electrospinning Process

In the electrospinning set-up (see Figure 4.1), a glass syringe was used to stock each of the as-prepared PS solutions. A 1-cm long blunt-end stainless-steel gauge 18 (OD = 1.2 mm) needle was used as the nozzle. The syringe was tilted ca. 45° from a horizontal baseline in order to maintain constant presence of a droplet at the tip of the needle. The feed rate of the solution was controlled by pressurized nitrogen gas through a flow meter. A piece of thick aluminum (Al) sheet was used as a screen collector. A Gamma High Voltage Research D-ES30PN/M692 power supply was used to charge the spinning PS solution by connecting the emitting electrode of either positive or negative polarity to the needle and the grounding one to the screen collector. Unless otherwise noted, the electrical field strength was varied (i.e. 1:1, 2:1, or 3:1 kV/cm), either by fixing the collection distance (i.e. 7 kV/7 cm, 14 kV/7 cm, or 21 kV/7 cm) or by fixing the applied voltage (i.e. 25 kV/25 cm, 25 kV/12.5 cm, or 25 kV/8.3 cm). In all of the spinning conditions, the collection time was fixed at about 15 seconds.

4.3.4 Characterization of as-Spun Fibers

Morphological appearance of the as-spun PS fibers was investigated using a JEOL JSM-5200 scanning electron microscope (SEM). Each specimen was coated with a thin layer of gold using a JEOL JFC-1100E ion sputtering device prior to observation under SEM. The average fiber diameter of the electrospun fibers was measured by Semafore 4.0 software from SEM images. The electrospinnability (e.g. the area of the as-spun fibers in two dimensions per unit area per unit time) of the as-spun PS fibers was investigated by using the Adobe Photoshop® CS software. SEM micrographs of PS fibers were converted to black and white images (threshold) by

adjusting the pixels until obtained the certain images (Hongrojjanawiwat *et al.*, [9]). A thermo Nicolet Nexus 670 Fourier-transformed infrared spectroscope (FT-IR) was used to characterize the as-spun PS fibers whether they contained appreciable amount of solvent molecules using the KBr-pellet technique. The electrospinnability of the as-spun PS fibers was quantified by number of fibers on SEM images obtained.

4.4 Results and Discussion

4.4.1 Effect of Solvent Properties and Solution Parameters

In order to study the effect of solvent on the electrospinnability of the resulting PS solutions, SEM images of as-spun fibers obtained from 10% w/v PS solution in each of the single solvents used were analyzed. In this case, the electrospinnability was assessed by the amount of as-spun fibers (pixels of as-spun fibers on the SEM images) per unit area (i.e. the pixels of as-spun fibers divided by the total pixels of the SEM image investigated). Based on the analyses, the electrospinnability of the resulting solution of PS in DMF was found to be the best, followed by that of the solution in DCE, MEK, and EA, respectively.

The effect of solvent on electrospinnability of the resulting PS solutions in DMF, DCE, MEK, and EA is to be discussed further against some influencing properties of the solvent. Figure 4.2 shows overlay plots of the electrospinnability and the property value (i.e. molecular weight, boiling point, density, dipole moment, dielectric constant, difference in solubility parameters between that of the solvent and the PS solute molecules, viscosity, conductivity and surface tension) of the solvents. Obviously, the electrospinnability of the spinning PS solution or the electrospinnability of the as-spun fibers correlated well with the boiling point, dipole moment, dielectric constant, difference in the solubility parameters between that of the solvent and the PS solute molecules, and viscosity, respectively.

As can be seen, the solvent having or providing a high boiling point, high dipole moment, high dielectric constant, high difference in the solubility parameters between that of the solvent and the PS solute molecules, and viscosity

gave the best candidates for electrospinning of the resulting solution. Tables 4.2 to 4.4 summarize the viscosity, surface tension, and conductivity of both pure solvent and the resulting PS solutions. Interestingly, while the electrospinnability of the resulting solutions did not correlate well with both the conductivity and the surface tension values, but it exhibited a strong correlation with the viscosity value, of the solutions.

4.4.2 Effect of Single Solvent

4.4.2.1 *1,2-Dichloroethane (DCE)*

DCE was able to dissolve PS pellets to form a clear solution within two days. The viscosity of 10%, 20%, and 30% (w/v) PS solutions in DCE was found to increase from that of the pure solvent (i.e. 0.73 cP) to be 28.8, 171, and 1574 cP, respectively (see Table 4.2), while the surface tension was found to increase slightly from that of pure solvent (i.e. 32.5 mN/m^2) to be 33.2, 33.3, and 33.9 mN/m^2, respectively (see Table 4.3). The spinning of the PS solutions in DCE was very easy, most likely due to the relatively high dipole moment that the solvent exhibits (i.e. 2.94 Debye, see Table 4.1) and the rather low conductivity value of the solvent (i.e. 0.70 μS/cm, see Table 4.4). The SEM images of the electrospun fiber, shown in Figure 4.3, revealed that, at 10% (w/v), a large amount of smooth fibers and beaded fibers was obtained. Interestingly, for a fixed applied voltage of 25 kV, both the fiber and bead density observed were found to decrease with increasing collection distance and, for a fixed collection distance of 7 cm, both the fiber and bead density decreased with increasing applied voltage (see Figure 4.4). With increasing the concentration of the solution to 20% (w/v), very small amount of beads was present. Obviously, for a fixed applied voltage of 25 kV, the amount of beads was found to decrease with increasing the collection distance from 8.3 to 25 cm. At 20% (w/v), for a fixed collection distance of 7 cm, no jet was observed when the applied voltage was below 21 kV. Under these conditions, electrospun PS fibers could not be obtained. Interestingly, at the applied electrostatic field strength of 14 kV/7 cm, the obtained fibers were fused to adjacent ones. With further increase the concentration of the solution to 30% (w/v), only smooth, bead-less fibers were obtained. In a similar manner, for a fixed applied voltage of 25 kV, the density of

the fibers was found to decrease with increasing collection distance, and, for a fixed collection distance of 7 cm, the density of the fibers was found to decrease with increasing applied voltage.

4.4.2.2 *N,N-Dimethylformamide (DMF)*

DMF was able to dissolve PS pellets to form a clear solution within only 6 hours. The viscosity of 10%, 20%, and 30% (w/v) PS solutions in DMF was found to increase from that of the pure solvent (i.e. 0.85 cP) to be 25.40, 217, and 1016 cP, respectively (see Table 4.2), while the surface tension was found to increase slightly from that of pure solvent (i.e. 35.47 mN/m^2) to be 35.92, 35.87, and 35.72 mN/m^2, respectively (see Table 4.3). The spinning of the PS solutions in DMF was extremely easy, due possibly to the relatively high dipole moment value of 3.82 Debye and the relatively high conductivity value of 6.72 μS/cm of the solvent. In Figure 4.5, at 10% (w/v), very large amount of smooth and beaded fibers was observed. Apparently, for a fixed applied voltage of 25 kV, the amount of the bead was found to decrease with increasing collection distance. For a fixed collection distance of 7 cm, the amount of bead was found to decrease with increasing applied voltage. With increasing the concentration of the solution to 20% (w/v), very small amount of beads was present (as shown in Figure 4.5). Obviously, for a fixed collection distance of 7 cm, the amount of beads was found to decrease with increasing the applied voltage from the 7 to 21 kV. At 30% (w/v), only smooth as-spun fibers were observed (see Figure 4.6(g-i) and 4.6(g-i)).

4.4.4.3 *Ethylacetate (EA)*

EA was able to dissolve PS pellets to form a clear solution within three days. The viscosity of 10%, 20%, and 30% (w/v) PS solutions in EA was found to increase from that of the pure solvent (i.e. 0.56 cP) to be 18.40, 186, and 1423 cP, respectively (see Table 4.2), while the surface tension was found to decrease from that of pure solvent (i.e. 24.66 mN/m^2) to be 24.20, 23.86, and 23.52 mN/m^2, respectively (see Table 4.3). The spinning of the PS solutions in EA was quite easy to be spun, most likely due to the fair dipole moment value of 1.78 Debye and the conductivity value of 0.7 μS/cm. Evidently, both smooth and beaded fibers were observed for 10% (w/v) PS solution. With increasing the concentration of the

solution to 20% (w/v), a very small amount of beads was present. According to Figure 4.7, for a fixed applied voltage of 25 kV, the amount of beads decreased with increasing the collection distance from 8.3 to 25 cm. At 30% (w/v), only smooth as-spun fibers were observed. Interestingly, at low collection distance, the obtained fibers were fused to adjacent ones. In Figure 4.8, for a fix collection distance of 7 cm, the amount of beads decreased with increasing the applied voltage from 7 to 21 kV. At 10% (w/v), for a fixed collection distance of 7 cm, no jet was observed when the applied voltage was lower than 14 kV. Obviously, at 10% (w/v), only discrete beads or half-hollowed spheres (HHS) were observed. The diameter of the beads ranged between 20 and 35 μm. Fong *et al.* [10] reported that the formation of ribbon shaped fibers was caused by the evaporation of the solvent. Bongnitzki *et al.* [11], on the other hand, reported that the observed porous structure was cause by the electrospinning process itself.

4.4.2.4 *Methylethylketone (MEK)*

MEK was able to dissolve PS pellets to form a clear solution within one day. The viscosity of 10%, 20%, and 30% (w/v) PS solutions in MEK was found to increase from that of the pure solvent (i.e. 0.56 cP) to be 16.8, 158, and 696 cP, respectively (see Table 4.2), while the surface tension were found to decrease from that of pure solvent (i.e. 24.39 mN/m^2) to be 23.48, 23.07, and 22.85 mN/m^2, respectively (see Table 4.3). The spinning of the PS solutions in MEK was easy most likely due to the relatively high dipole moment that the solvent shows (i.e. 2.76 Debye, see Table 4.1) and the fair conductivity value of the solvent (i.e. 0.92 μS/cm, see Table 4.4). At 10% (w/v), very large amount of smooth and beaded fibers was observed. The beads were completely disappeared when the concentration of the solution increased to 20% and 30% (w/v). At such concentrations, for a fixed applied voltage of 25 kV, the size of the beads was found to increase with increasing collection distance as shown in Figure 4.9. In Figure 4.10, for a fixed collection distance of 7 cm, the size of the beads was found to increase with increasing the applied voltage. With further increase in the concentration of the solution (20%, and 30% (w/v)), for a fixed applied voltage of 25 kV, the density of the fibers was found to increase with increasing collection

distance, and, for a fixed collection distance of 7 cm, the density of the fibers was found to decrease with increasing applied voltage. The obtained fibers were fused to adjacent fibers, most likely a result of the less time for solvent evaporation prior to deposition on the collector plate.

4.4.3 Effect of Concentration

Solution properties (i.e. viscosity, conductivity, and surface tension) have been shown to have a significant effect on the morphological appearance of as-spun fibers. However, viscosity, and surface tension also play important roles in determining the range of concentrations from which continuous fibers can be obtained. At low viscosities, surface tension is the dominant factor influencing the fiber morphology and below a certain concentration drops will form instead of fibers. At high concentrations, processing will be prohibited by an inability to control and maintain the flow of a polymer solution to the tip of the needle and by the cohesive nature of the high viscosity solution. In this study, the electrospinning was carried out on PS having a MW of about 300,000 Da at the concentration ranging between 10 and 30% (w/v). The viscosity of these solutions ranged between 16.80 and 1574 cP and the surface tension of these solutions ranged between 22.9 and 35.9 mN/m^2 (Figure 4.11).

In electrospinning, six types of force are involved: they are i) body or gravitational force, ii) electrostatic force which carries the charged jet from the needle to the collector screen, iii) Coulombic repulsion force which tries to push apart adjacent charged species being present within the jet segment and is responsible for the stretching of the charged jet during its flight to the target, iv) viscoelastic force which tries to prevent the charged jet from being stretching, v) surface tension also acts against the stretching of the surface of the charge jet, and vi) drag force from the friction between the charged jet and the surrounding air (Wannatong *et al.*, [12]). Due to the combination of these forces, the electrically charged jet travels in a straight trajectory for only a short distance before undergoing a bending instability, which results in the formation of a looping trajectory. During its flight to the collector screen, the charged jet thins down, at the same time, dries out or solidifies to leave fibers on the collector screen. At lower concentrations or

viscosities, the viscoelastic force was comparatively smaller than the Coulombic repulsion force. This results in the over-stretching of a charged jet, hence the break-up of the charged jet into many small spherical droplets results.

Changing the polymer concentration could alter the solution viscosity, as shown in Table 4.2. A series of samples of varying PS concentrations was electrospun, resulting in diverse morphologies. A critical concentration needed to be exceeded in the electrospinning process as extensive chain entanglement is necessary requirement for obtaining electrospun fibers. In electrospinning, the coiled macromolecules were stretched along the extensional flow field; a result of the Coulombic repulsion that caused the ejected, charged jet to elongate and, after solidification, ultrafine fibers resulted. Below this concentration, chain entanglements were insufficient to stabilize the jet and the contraction of the jet driven by the surface tension caused the formation of beads or beaded fibers. At higher concentrations, the viscoelastic force was large enough to inhibit the stretching of the jet. The fiber shape was more uniform as a result. However, when the concentration was too high, the spinnability of the solution diminished as the jet could clog up very rapidly at the tip of the nozzle.

At low concentrations or viscosities, the viscoelastic force (i.e. a result of the low degree of chain entanglements) in a given jet segment was not large enough to counter the greater Coulumbic force, resulting in the break-up of the charged jet into smaller jets, which, as a result of the surface tension, were later rounded up to form droplets. This phenomenon has been familiarized in the industries as the electrospraying process and has commonly been used in many applications such as paint spraying, powder coating, and so on.

At higher concentrations or viscosities, the charged jet did not break up into small droplets, a direct result of the increased chain entanglements (i.e. hence an increase in the viscoelastic force) that were sufficient to prevent the break-up of charged jet and to allow the Coulombic stress to further elongate the charged jet during its flight to the grounded target which ultimately thinned down the diameter of the charged jet. However, if the concentration was not high enough (i.e. 10% (w/v)), a combination of smooth fibers and minute, discrete droplets was observed. A slight increase in the concentration of the solution to 20% (w/v) resulted in the

disappearance of the minute, discrete droplets, leaving only a combination of smooth and beaded fibers on the target. With further increasing concentration (or viscosity) of the solution, the number of beads along the fibers was found to decrease and their shape appeared to be more elongated. When the concentration of the solution increased to 30% (w/v), beads were disappeared altogether, leaving only smooth ultrafine fibers on the target. Some phenomenon can occur at higher concentrations such as wet fibers. Kenavy *et al.* [13] reported rather thick poly(ethylene-co-vinyl alcohol) fibers being observed from the 15 and 20% (w/v) solutions appeared to be fused at overlapping junctions, perhaps the result of the incomplete solvent evaporation.

One important question is whether solvent was present in the as-spun fibers obtained. In order to find an answer to such a question, FT-IR was used to characterize some of the as-spun PS fibers. Figure 4.12 illustrates IR spectra of PS fibers at different concentration and different type of solvents. Table 4.5 summarizes some important peak assignments from FT-IR spectra of as-spun PS fibers. Obviously, the absorption peaks observed only belonged to those of PS, with no other assignments belonging to those of the solvents used being observed. The results confirmed complete vaporization of the solvent. In addition, the process did not affect the chemical integrity of the resulting as-spun fibers.

4.4.4 Effect of Electrical Field Strength

The electrospinning of PS solutions in various solvent were carried out under various applied electrical field strengths (i.e. 1:1, 2:1, or 3:1 kV/cm) either by fixing the collection distance (i.e. 7 kV/7 cm, 14 kV/7 cm, or 21 kV/7 cm) or by fixing the applied voltage (i.e. 25 kV/25 cm, 25 kV/12.5 cm, or 25 kV/8.3 cm).

4.4.4.1 *Effect of Applied Voltage*

In the electrospinning process, the shape of the initiating droplet on the exit opening of the electrode can be changed by several electrospinning parameters such as applied voltage, and viscosity of the polymer solution. When increasing in the electrospinning voltage can alter the shape of the initial droplet. Consequently, the resulting fiber morphology can be changed from a typical cylindrical shape to a beaded or fiber structure. The electrical field effect can

be understood by the following argument. The jet initiation is a self-accelerating process. Once an electric field is applied on the droplet of the polymer solution at the tip of the spinneret, the surface of the liquid becomes charged via the motion of ions through the liquid. When the electric force overcomes the surface tension, electrically charged jet is ejected.

For example, for 10 % (w/v) PS solutions in every type of solvent at collection distance of 7 cm, the fiber diameter of as-spun fibers under different applied voltages (7, 14, and 21 kV) is summarized in Figure 4.13. At 7 kV, the diameter of the droplet was found to be larger than the opening diameter of the spinneret. The jet was initiated from the droplet suspended at the end of the spinneret. The hemispherical surface of the solution was elongated to from a conical shape (Taylor Cone). The Taylor cone was maintained even when the feed of the PS solution to the tip of the spinneret was faster than the jet could carry the fluid away. The resulting fibers are shown in Figure 4.4a, 4.6a, 4.8a, and 4.10a. When the applied voltage was increased (i.e. to 14 kV), the jet velocity was increased and the solution was removed from the tip more quickly. As the volume of the droplet on the spinneret became smaller, the Taylor cone shape oscillated and became asymmetrical at 21 kV. Under this condition, beaded fibers were prone to form. The diameter of the beaded fibers was found to be smaller and the average distance between the beads on the fibers became shorter at further increase in voltage. Conclusively, the fibers appeared to be larger with increasing applied voltage and concentration of the spinning PS solution.

A lower distribution of the diameters was observed at applied voltage of 7 kV, while a broader distribution of the diameters was obtained at higher voltage of 21 kV. These results can be explained based on the relationships among the three major forces (i.e. Coulumbic repulsion force, viscoelastic force, and surface tension) influencing the fiber diameters. At a low applied voltage (i.e. 7 kV), the Coulombic force was not high when compared with that of the surface tension. This resulted in the as-spun fibers with large diameters and the presence of large beads along the obtained fibers. At moderate applied voltages (i.e. 14 kV), all of the three forces were well-balanced, resulting in a lower distribution of the fiber diameters. With further increase in the applied voltage (i.e. 21 kV), the columbic force was

greater than that of the viscoelastic force. This might result in an increased possibility for the breakage of an over-stretched charged jet during their flight to the target. There is both longitudinal and transverse stretching: the latter leads to the increasing in the fiber diameter. Moreover, with increasing applied voltage, a charged jet travels to the grounded target much faster. The solvent, therefore, has less time to evaporate. Retraction of the charged jet can then occur as soon as some of the charges carried in the jet are neutralized (causing the reduction in the Coulombic force), which, finally leads to the bigger, but irregular fibers.

4.4.4.2 *Effect of Collection Distance*

For a fixed applied voltage of 25 kV, the fiber diameter was found to decrease with increasing collection distance, which was thought to be due to the great extent of bending instability. The bending instability signifies the total path length of a jet segment during its flight to the grounded target. The longer path length means the greater probability for the jet segment to thin down as a result of the Columbic repulsion. According to Figure 4.14, diameter of the as-spun fibers generally increased with increasing concentration of the solutions. Due to an increase in the viscosity, the viscoelastic force increased, hence the greater resistance towards the thinning of the fiber diameter. The increase in the viscosity of the solution also resulted in a decrease in the total path length, which, in turn, accented the observed increase in the fiber diameter.

4.4.5 Effect of Emitting Electrode Polarity

Figures 4.15 and 4.16 summarized the diameters of the as-spun PS fibers under the negative polarity of the emitting electrode at various electrostatic field strengths by fixing the collection distance (i.e. 7 kV/7 cm. 14 kV/7 cm, and 21 kV/7 cm) and by fixing the applied voltage (i.e. 25 kV/25 cm. 25 kV/12.5 cm, and 25 kV/8.3 cm), respectively. Comparatively to the fibers obtained under the positive polarity, fibers with larger diameters were obtained, most likely a result of the difference in the nature of the concentration of charge carriers present within a jet segment under different polarities of the emitting electrode that resulted in the difference in the mass flow rate (a result of the higher charge density) and for the

formation of flat fibers might be the collapsing of the dried skin layer of a jet after the solvent inside the jet had evaporated (Koombhongse *et al.*, [14]).

4.4.6 Effects of Ionic Salt Addition

As we intend to use the electrospun fibers for many applications, such as soldier protective clothing (Gibson *et al.*, [15]), filtering, drug delivery (Doshi *et al.*, [3]), wound dressings, and composite reinforcement (Doshi *et al.*, [3]), it is important to investigate the effects of salt addition on the resulting morphologies of the as-spun fibers. In this section, it is demonstrated that very different morphologies of the electrospun fibers could be obtained when different salts were added into PS solutions for electrospinning. The low concentration of salt used was to ascertain complete solubility of the salt in the solutions.

Figure 4.17 summarizes viscosity, conductivity, and surface tension of the salt-loaded PS solutions. Obviously, addition of 1% w/v LiCl or KCl salt resulted in remarked reduction in the viscosity and significant increase in the conductivity, while it had no effect on the surface tension, of the resulting solutions. The morphological appearance of the as-spun fibers is shown in Figure 4.18. Obviously, the addition of 1% (w/v) LiCl or 1% (w/v) KCl salt resulted in fibers of larger diameter. This simply means that both the electrostatic and the Coulombic forces should be increased with added salt. Intuitively, the increase in the Coulombic stretching force should result in the reduction in the obtained fiber diameter (coupled with the observed reduction in the viscoelastic force with the salt addition), but the results shown in Figure 14 suggest otherwise. The otherwise increase in the fiber diameter with added salt could be a result of the increase in the mass flow (due to the increase in the electrostatic force acting on a jet segment) as well as the expected decrease in the total path length (due also to the increase in the electrostatic force). Doshi *et al.* [3] also reported that the addition of a small amount of salt resulted in the dramatic increase in the mass flow and a decrease in the viscosity, which resulted in fibers with large diameters when triethylbenzyl ammonium chloride was added into the solution of polyurethaneurea in DMF.

Further data analyses revealed that, the different salts showed different effects on the final diameter of the fibers. The fibers electrospun from 30% w/v PS

solution with 1% w/v LiCl salt addition exhibited the diameter ranging from around 30.1 to 35.9 μm, while the fibers electrospun from the solution with 1% w/v KCl exhibited the diameter in the range of 31.1 to 36.2 μm (Figure 4.19). This effect can be understood as follows. Besides the density of the charges carried by the jet, the size of the ions has an important impact on the resulting fiber diameter. Ions with smaller atomic radius have a higher charge density and thus a higher mobility under an external electric field. In this work, lithium has smaller radius than potassium. Thus the elongational forces imposed on the jet with lithium should be higher than that with potassium. Therefore, the electrospun fibers from the PS solution with 1% (w/v) LiCl showed the smaller average fiber diameter than the fibers spun from solution with 1% (w/v) KCl.

It is hypothesized that both the application of the negative polarity and the addition of 1%(w/v) salt help increase the mass flow rate, hence an increase in the size of the fibers obtained with the flat shape being formed by the much slower evaporation rates as a result of the larger size of the fibers.

4.4.7 Effect of Mixed Solvent

Since PS can be dissolved in DMF within 6 hours into a clear solution and the resulting solution showed the best spinnability among the use of all other solvents investigated, DMF was then used as the main solvent to study the effect of mixed solvent on the morphology and size of the resulting as-spun PS fibers. In mixed solvent systems, various solvents (i.e. DCE, EA, and MEK) were mixed with DMF in various volumetric ratios (i.e. 75/25, 50/50, and 25/75). The resulting solutions were tested for viscosity, surface tension, and conductivity and the results are summarized in Table 4.6.

4.4.7.1 *DMF:DCE*

Both the viscosity and the conductivity were found to decrease with increasing DCE content, while the surface tension was almost unaffected (see Table 4.6). SEM images of as-spun PS fibers from mixed solvent between DMF and DCE of various compositional ratios are shown in Figure 4.20. Obviously, discrete fibers with smooth surface were observed from 20 and 30%

(w/v) PS solutions (i.e. viscosity ranging between 202 and 1136 cP) in every compositional ratio, while fused fibers were obtained from 30% (w/v) PS solutions in mixed solvent with the compositional ratio of 75/25. The fused fibers obtained should be a direct result of the high boiling point of the mixed solvent and the large size of the fibers observed. Fused fibers were also observed from the electrospinning of PCL in a mixture of methylene chloride and toluene (Lee *et al.*, [7]). Alteration of the physico-chemistry of the polymer in mixed solvent of different compositional ratios could be also a factor affecting the spinnability of the solution as well as the final morphology of the as-spun fibers. Obviously, the average fiber diameter was found to decrease with increasing DCE content, most likely a result of the observed decrease in the viscosity of the resulting solutions.

4.4.7.2 *DMF:EA*

Due to the desirable low boiling point and low surface tension of EA for electrospinning, it was chosen as an adjusting solvent to be mixed with DMF in various volumetric ratios (i.e. 75/25, 50/50, and 25/75). Obviously, the viscosity increased from that of pure DMF with addition of EA, but it decreased monotonically with further increase in the EA content. On the other hand, the surface tension decreased monotonically from that of pure DMF with addition of and increasing amount of EA. Quantitative analysis of the as-spun PS fibers revealed that diameters of the fibers decreased initially with increasing EA content up to about 50% v/v and, with further increase in the EA content, the fiber diameters increased. SEM images of the as-spun fibers from PS solutions in mixture of DMF and EA as shown in Figure 4.21 showed that whenever the size of the as-spun fibers was relatively large, fused fibers were obtained.

4.4.7.3 *DMF:MEK*

Due to the lowest surface tension of MEK in comparison with other solvents investigated in this work. Both the viscosity and the surface tension of the resulting solutions were found to decrease monotonically with increasing MEK content. SEM micrographs of as-spun fibers from PS solutions in DMF and MEK of various compositional ratios are shown in Figure 4.22. The smooth fibers or the fiber without beads were observed for the increasing the MEK content, while fused fibers were obtained from 30% (w/v) PS solution at the ratio of DMF and MEK of

50/50 and 25/75, respectively. As a result, the average fiber diameter was found to decrease with increasing MEK content.

4.5 Conclusions

The electrospinning technique was used to produce PS fibers. PS solutions were prepared in both single solvent systems and mixed solvent systems. The effects of solution properties and process condition on the fiber diameter and morphological appearance of the submicron PS were thoroughly investigated. Results demonstrated that the morphology of electrospun polymer fibers strongly depended on the processing conditions and solvent systems. It was shown that higher viscosity (i.e. concentration) and higher applied voltage favoured the formation of uniform fiber with no bead-on-string structure. On the other hand, an increasing the collection distance resulted in the thinner of fiber. Mixing DMF with second solvent (i.e. DCE, EA, and MEK) to serve as a mixed solvent for PS caused the resulting solutions to have lower viscosity, and lower surface tension which resulted in the smaller fiber diameters obtained. Lastly, addition of some inorganic salts to the solution resulted in an increase in the conductivity values, which, in turn, caused the fiber diameters to increase due to the much increase in the mass flow (i.e. low viscosity).

4.6 Acknowledgements

The authors acknowledge partial supports received from the petroleum and Petrochemical Technology Consortium (through a Thai government loan from the Asia Development Bank), Chulalongkorn University (through a grant from the Ratchadapesak Somphot Endowment Fund for the foundation of the Conductive and Electroactive Polymers Research Unit), the Thailand Research Fund-Master Research Grant (TRF-MAG), and the Petroleum and Petrochemical College, Chulalongkorn University.

4.7 References

[1] Z.M. Huang, Kotaki, Y.Z. Zhang, M. Kotaki, S. Ramakrishna. *Composite Science and Technology* **2003**, 63, 2223.

[2] J.M. Deitzel, J.D. Kleinmeyer, J.K. Hirvonen, T.N.C. Beck. *Polymer* **2001**, 42, 8163.

[3] J. Doshi, D.H. Reneker. *Journal of Electrostatics* **1995**, 35, 151.

[4] A. Formhals. US Patent 1,975,504,1934.

[5] P.K. Baumgarten. *Journal of Colloid and Interface Science* **1971**, 36, 71.

[6] H. Fong, I. Chun, D.H. Reneker. *Polymer* **1999**, 40, 4585.

[7] K.H. Lee, H.Y. Kim, Y.M. La, D.R. Lee. *Polymer* **2003**, 44, 1287.

[8] T. Jarusuwannapoom, W. Hongrojjanawiwat, S. Jitjaicham, L. Wannatong, M. Nithitanakul, C. Pattamaprom, P. Koombhongse, R. Ramgkupan, P. Supaphol. *European Polymer Journal* **2005**, 41, 409.

[9] W. Hongrojjanawiwat, T. Jarusuwannapoom, P. Supaphol, R. Rangkupan, P. Koombhongse, and C. Pattamaprom. *Journal of Polymer Science – B: Polymer Physics*, submitted.

[10] H. Fong, W. Liu, CS Wang, R.A. Vaia. *Polymer* **2002**, 43, 775.

[11] B. Bongnitzki, W. Czado, T. Frese, A. Schaper, M. Hellwig, M. Streinhart, A. Griner, J.H. Wendorff. *Advanced Materials* **2001**, 13, 70.

[12] L. Wannatong, A. Sirivat, P. Supaphol. *Polymer International* **2004**, 53, 1851.

[13] E.-R. Kenawy, J.M. Layman, J.R. Watkins, G.L. Bowlin, J.A. Matthews, D.G. Simpson, G.E. Wnek, *Biomaterials* **2003**, 24, 907.

[14] S. Koombhongse, W. Liu, D.H. Reneker, Journal of polymer Science: Polymer Physics Edition ***2001***, 39, 2598.

[15] P.W. Gibson, I. Yilgor, B. Erman. *American Institute of chemical Engineers* **1999**, 45, 190.

Table 4.1 Properties of solvents used in this work

Solvents	Chemical formula	Molecular weight (g/mol)	Boiling point (°C)	Density (g/cm^3)	Dipole moment (Debye)	Dielectric constant	Solubility parameter $(MPa)^{1/2}$
DCE	$ClCH_2CH_2Cl$	99	83.5	1.239	2.94	10.19	20.2
DMF	$(CH_3)_2NCHO$	73.1	153	0.94	3.82	38.3	24
EA	$CH_3COOCH_2CH_3$	88.1	77.1	0.888	1.78	6.02	18.3
MEK	$CH_3CH_2COCH_3$	72.1	79.6	0.794	2.76	18.5	18.8

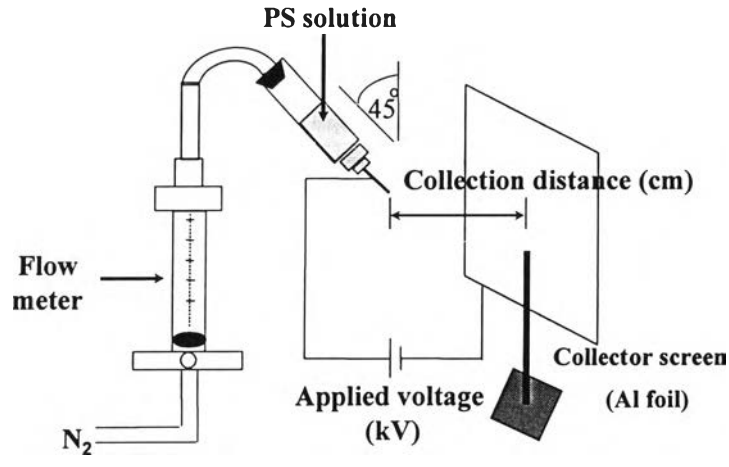

Figure 4.1 Experimental set-up for the electrospinning process of PS solution.

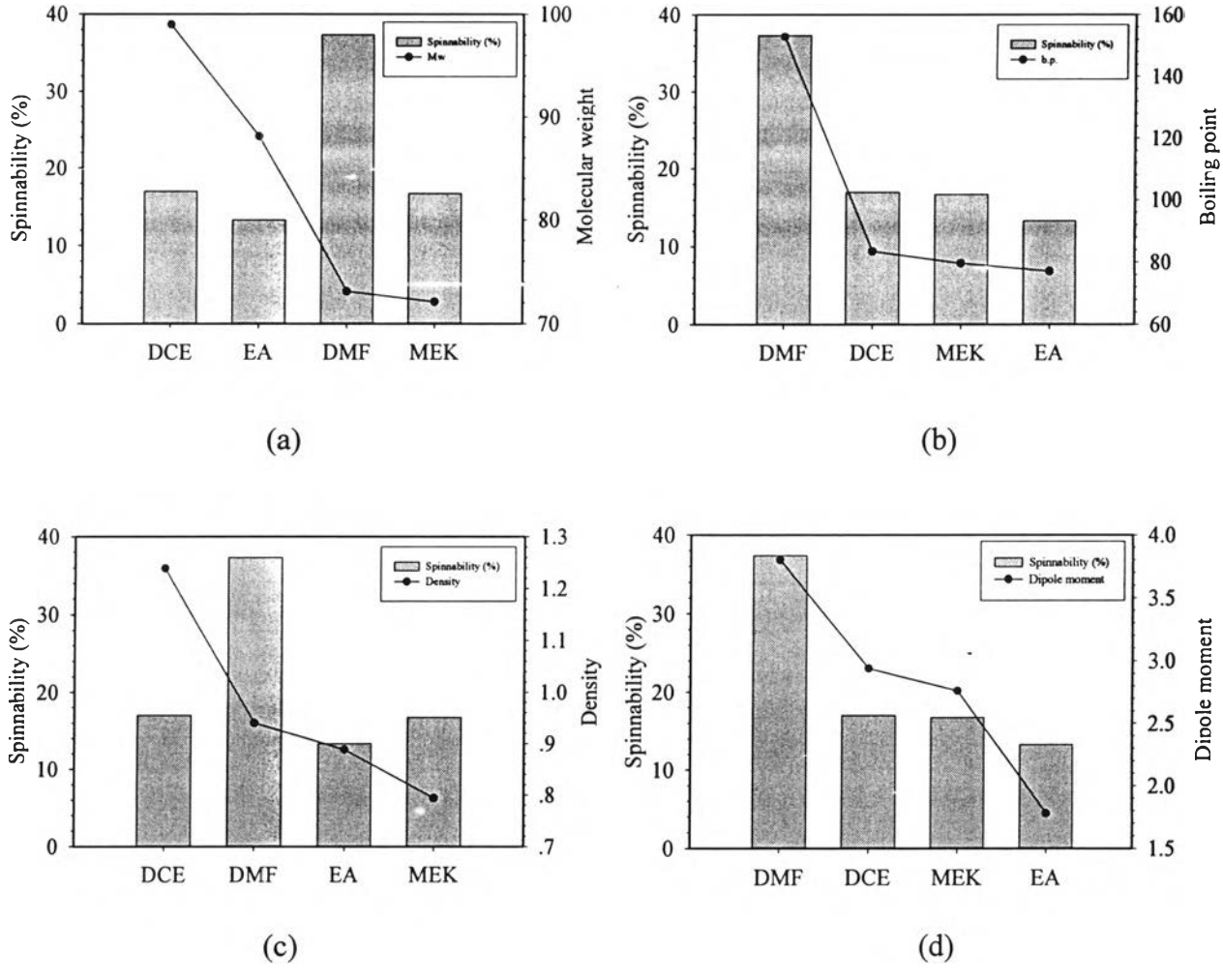

Figure 4.2 (a) Effect of molecular weight of the solvent on the spinnability. (b), (c), (d), (e), (f), (g), (h), and (i) are the effect of the boiling point, density, dipole moment, dielectric constant, different in solubility parameter, viscosity, conductivity, and surface tension of the solvent on the spinnability of 10% (w/v) PS as a function of four type different solvents. Applied electrical field was 25 kV/12.5 cm.

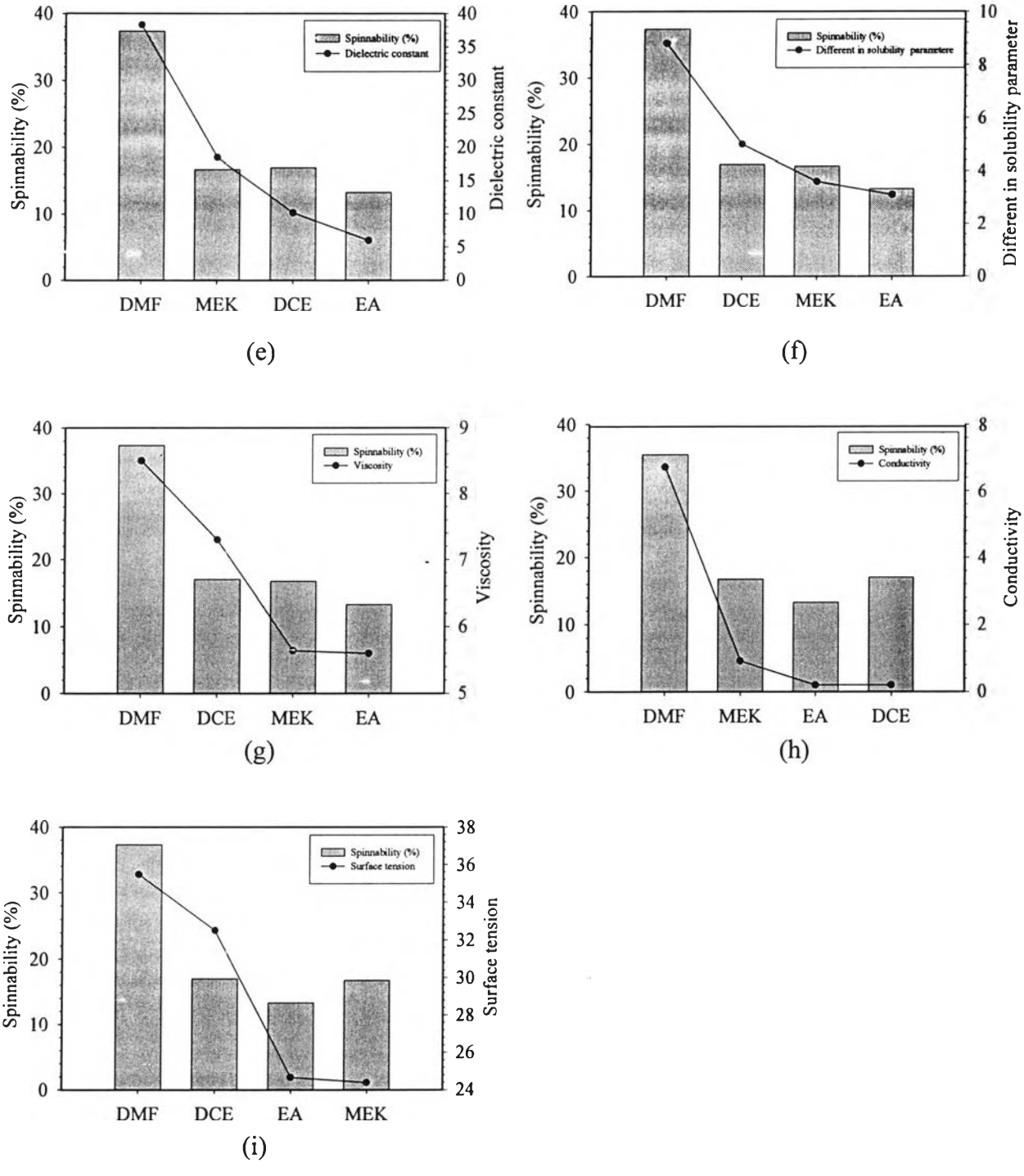

Figure 4.2(cont.) (a) Effect of molecular weight of the solvent on the spinnability. (b), (c), (d), (e), (f), (g), (h), and (i) are the effect of the boiling point, density, dipole moment, dielectric constant, different in solubility parameter, viscosity, conductivity, and surface tension of the solvent on the spinnability of 10% (w/v) PS as a function of four type different solvents. Applied electrical field was 25 kV/12.5 cm.

Table 4.2 Viscosity of solvents and as-prepared polystyrene solutions

Solvents	Viscosity (cP)			
	Pure Solvent	10% (w/v)	20% (w/v)	30% (w/v)
DCE	0.73	28.80	171	1574
DMF	0.85	25.40	217	1016
EA	0.56	18.40	186	1423
MEK	0.56	16.80	158	696

Table 4.3 Surface tension of solvents and as-prepared polystyrene solutions

Solvents	Surface tension (mN/m^2)			
	Pure Solvent	10% (w/v)	20% (w/v)	30% (w/v)
DCE	32.51	33.19	33.32	33.91
DMF	35.47	35.92	35.87	35.72
EA	24.66	24.20	23.86	23.52
MEK	24.39	23.48	23.07	22.85

Table 4.4 Conductivity of solvents and as-prepared polystyrene solutions

Solvents	Conductivity (μS/cm)			
	Pure Solvent	10% (w/v)	20% (w/v)	30% (w/v)
DCE	0.70	0.25	0.21	0.20
DMF	6.72	0.81	0.82	0.88
EA	0.70	0.04	0.04	0.05
MEK	0.92	0.45	0.48	0.40

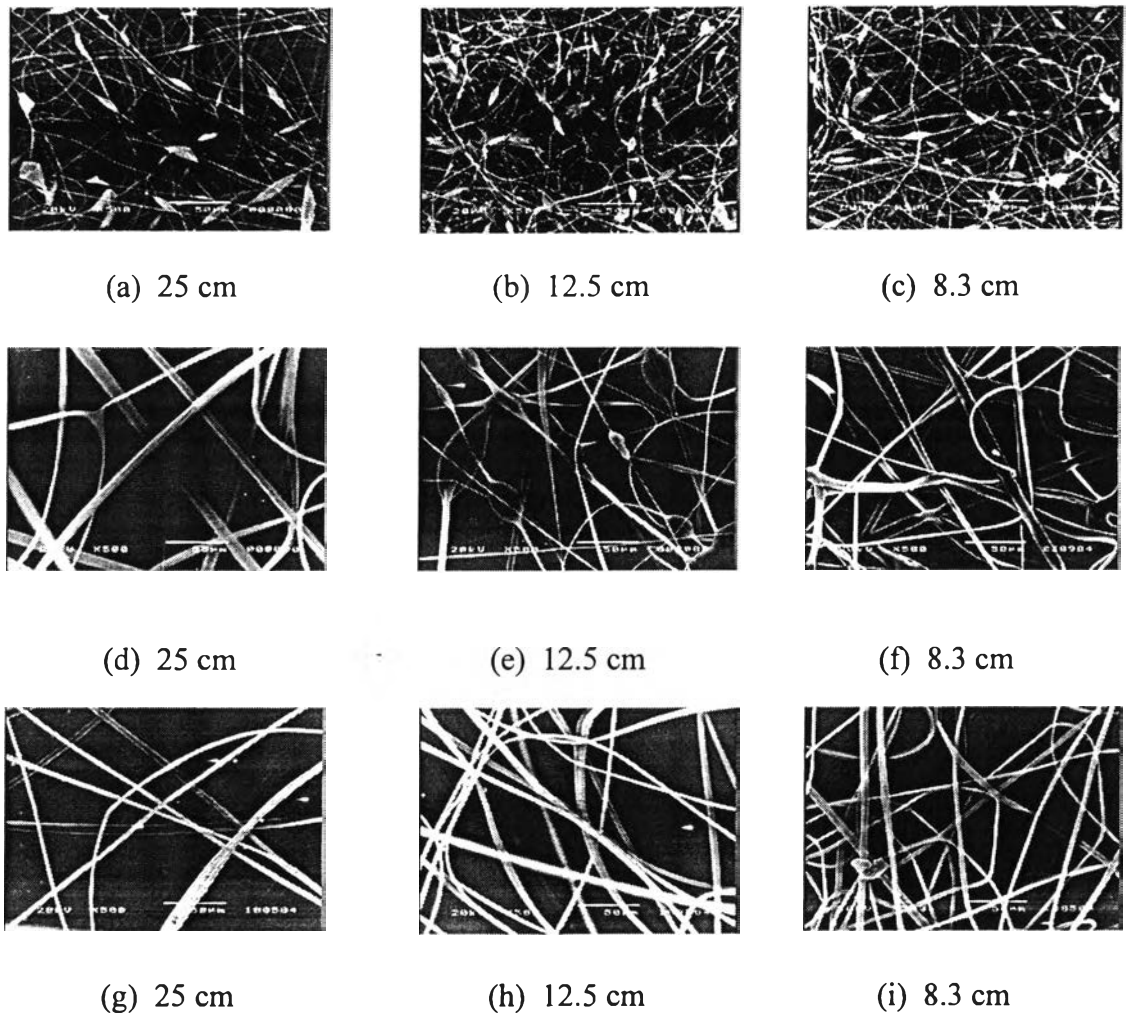

(a) 25 cm (b) 12.5 cm (c) 8.3 cm

(d) 25 cm (e) 12.5 cm (f) 8.3 cm

(g) 25 cm (h) 12.5 cm (i) 8.3 cm

Figure 4.3 SEM images (at a magnification of 500) of: (a-c) 10%; (d-f) 20%; (g-i) 30% (w/v) PS in DCE for effect of collection distance by fixing the applied voltage (i.e. 25 kV/25 cm, 25 kV/12.5 cm, and 25 kV/8.3 cm). Under positive polarity of the emitting electrode and the scale bar shown is for 50 μm.

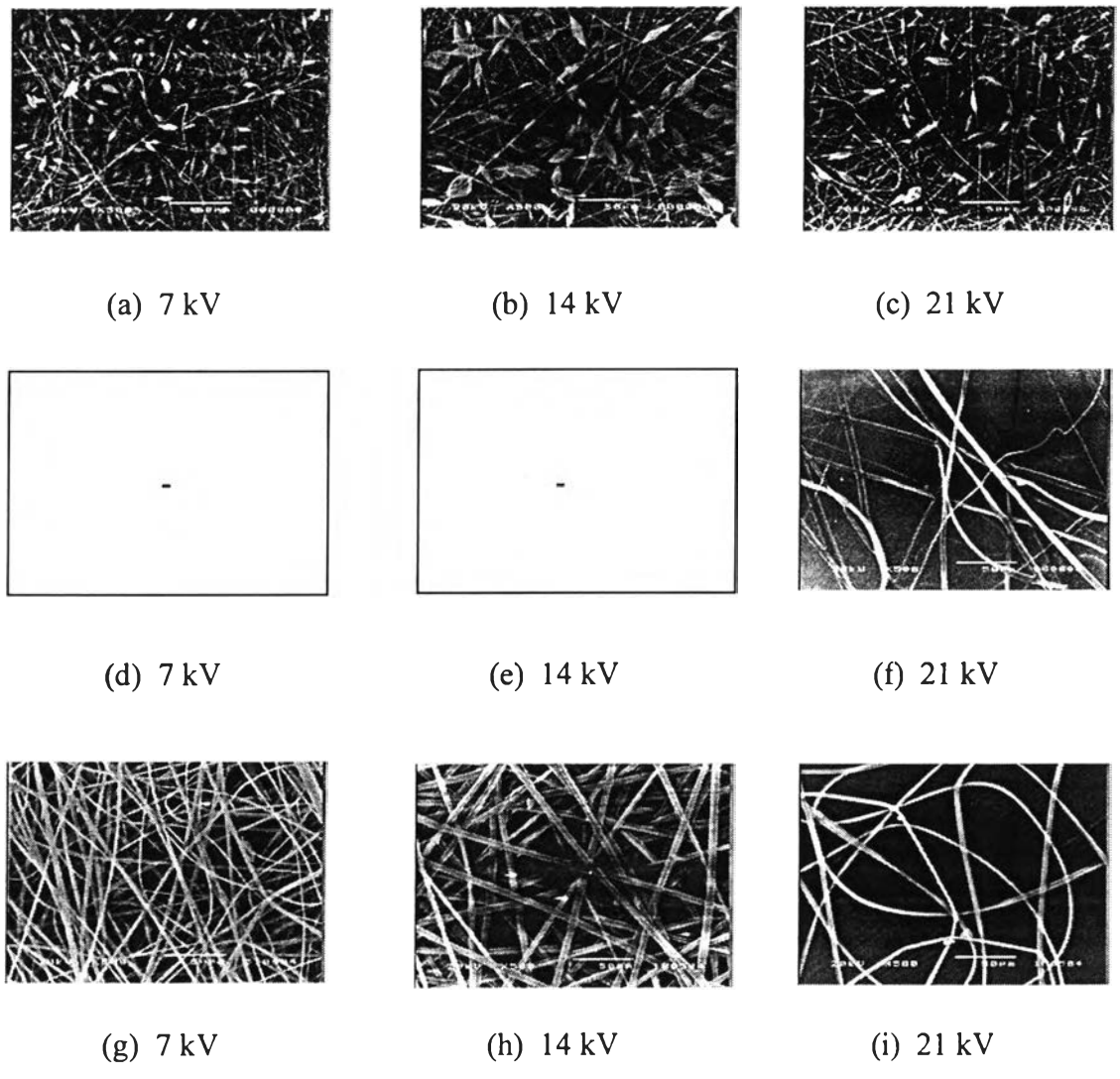

(a) 7 kV (b) 14 kV (c) 21 kV

(d) 7 kV (e) 14 kV (f) 21 kV

(g) 7 kV (h) 14 kV (i) 21 kV

Figure 4.4 SEM images (at a magnification of 500) of: (a-c) 10%; (d-f) 20%; (g-i) 30% (w/v) PS in DCE for effect of applied voltage by fixing the collection distance (i.e. 7 kV/7 cm, 14 kV/7 cm, and 21 kV/7 cm). Under positive polarity of the emitting electrode and the scale bar shown is for 50 μm.

Remark – means jet has not been found under this condition

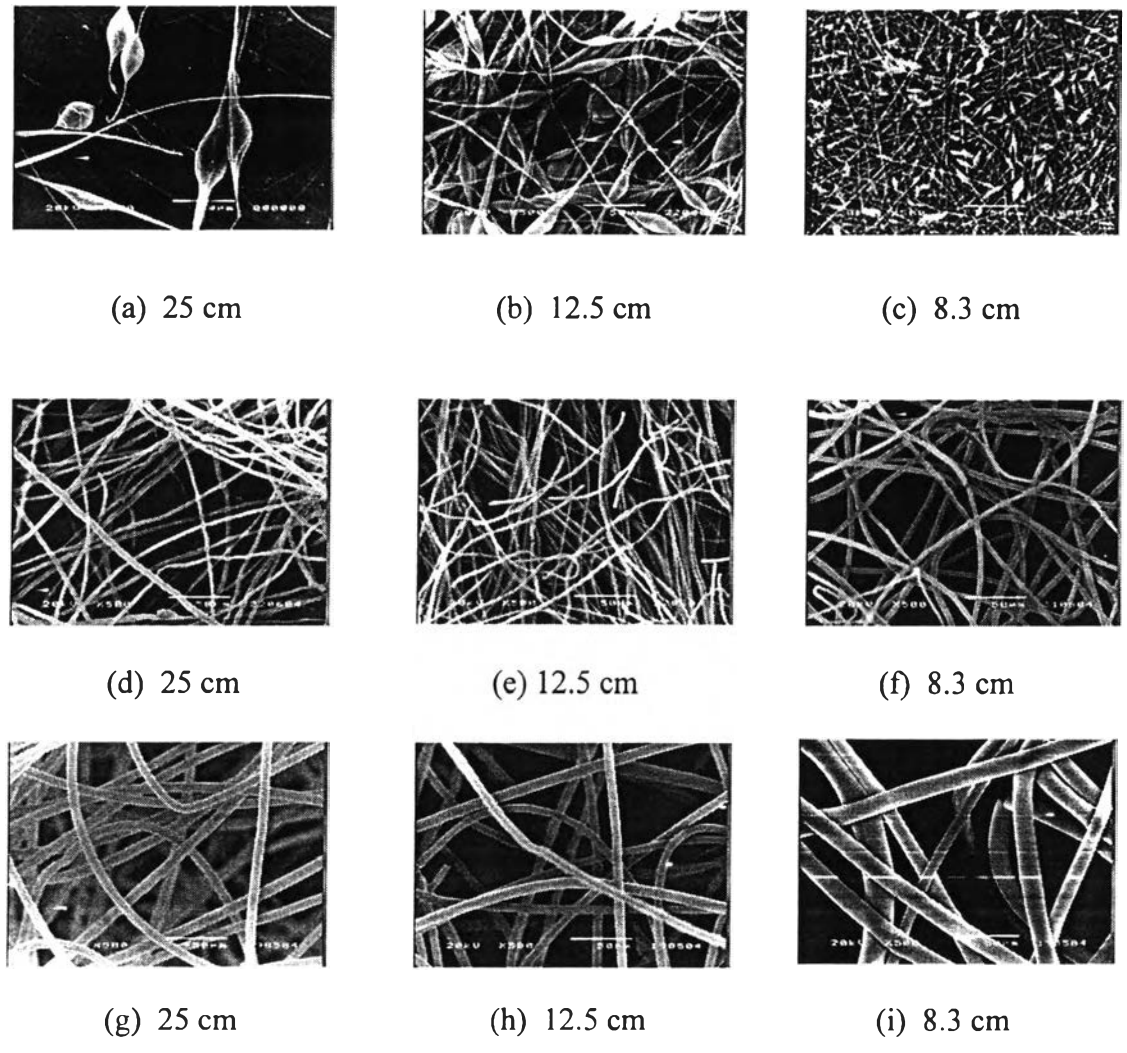

(a) 25 cm (b) 12.5 cm (c) 8.3 cm

(d) 25 cm (e) 12.5 cm (f) 8.3 cm

(g) 25 cm (h) 12.5 cm (i) 8.3 cm

Figure 4.5 SEM images (at a magnification of 500) of: (a-c) 10%; (d-f) 20%; (g-i) 30% (w/v) PS in DMF for effect of collection distance by fixing the applied voltage (i.e. 25 kV/25 cm, 25 kV/12.5 cm, and 25 kV/8.3 cm). Under positive polarity of the emitting electrode and the scale bar shown is for 50 μm.

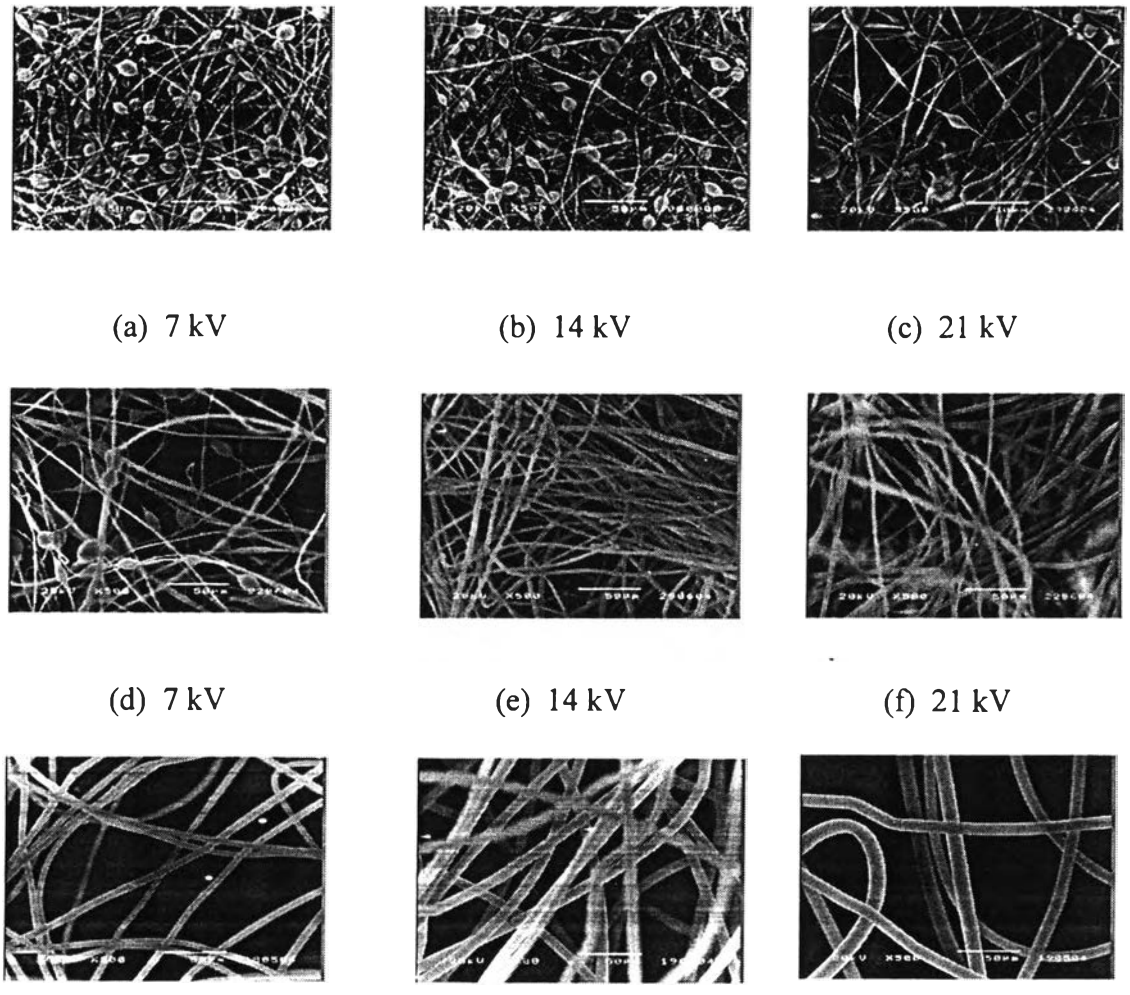

(a) 7 kV (b) 14 kV (c) 21 kV

(d) 7 kV (e) 14 kV (f) 21 kV

(g) 7 kV (h) 14 kV (i) 21 kV

Figure 4.6 SEM images (at a magnification of 500) of: (a-c) 10%; (d-f) 20%; (g-i) 30% (w/v) PS in DMF for effect of applied voltage by fixing the collection distance (i.e. 7 kV/7 cm, 14 kV/7 cm, and 21 kV/7 cm). Under positive polarity of the emitting electrode and the scale bar shown is for 50 μm.

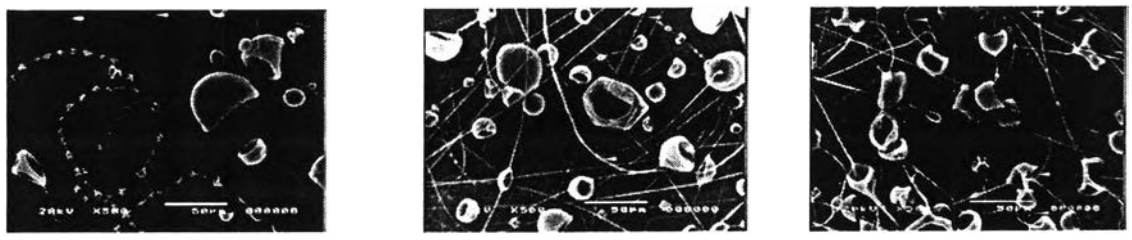

(a) 25 cm (b) 12.5 cm (c) 8.3 cm

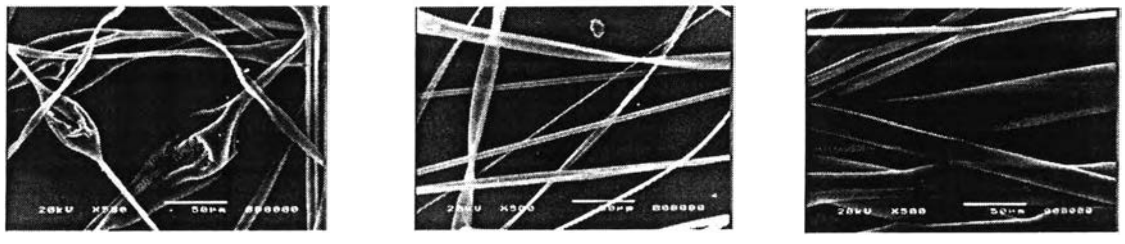

(d) 25 cm (e) 12.5 cm (f) 8.3 cm

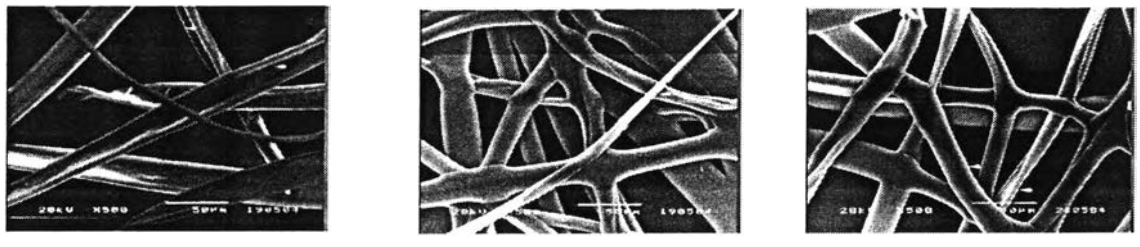

(g) 25 cm (h) 12.5 cm (i) 8.3 cm

Figure 4.7 SEM images (at a magnification of 500) of: (a-c) 10%; (d-f) 20%; (g-i) 30% (w/v) PS in EA for effect of collection distance by fixing the applied voltage (i.e. 25 kV/25 cm, 25 kV/12.5 cm, and 25 kV/8.3 cm). Under positive polarity of the emitting electrode and the scale bar shown is for 50 μm.

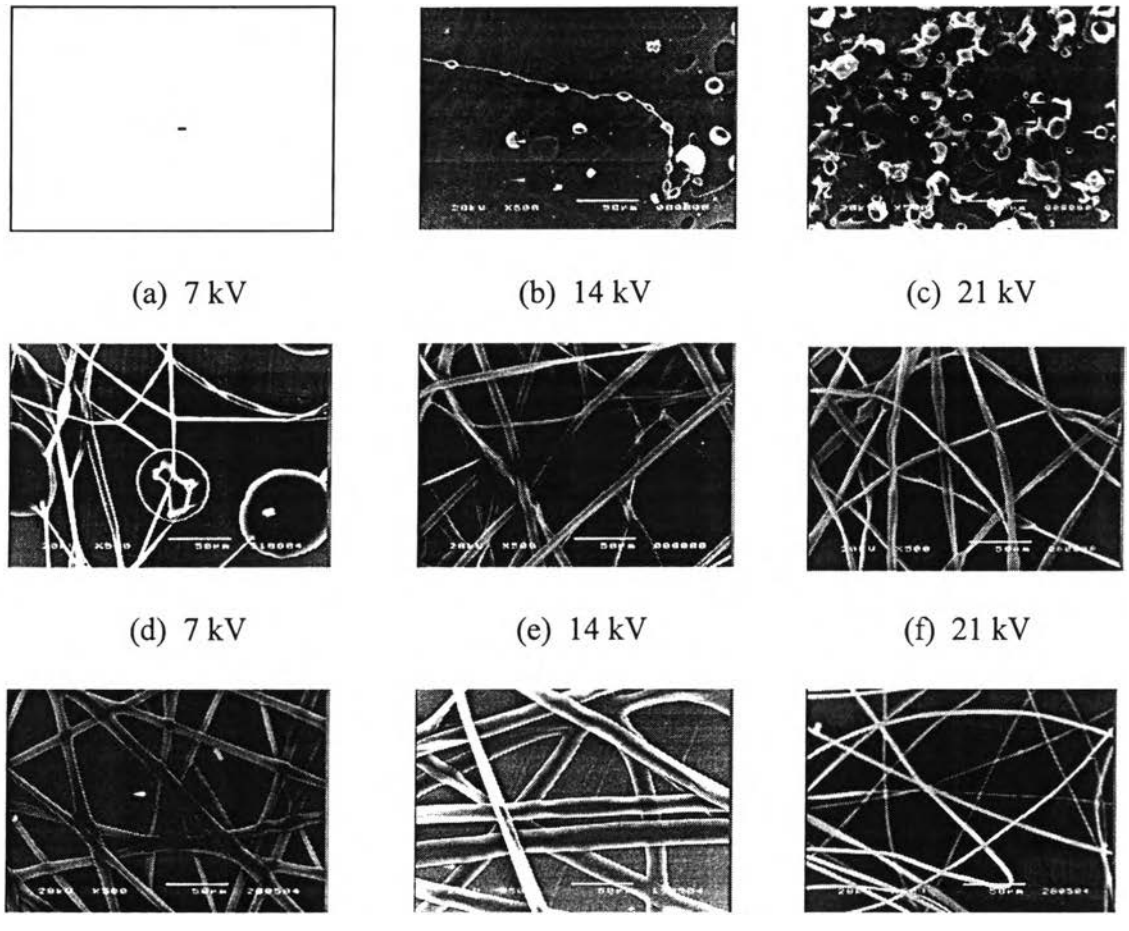

(a) 7 kV (b) 14 kV (c) 21 kV

(d) 7 kV (e) 14 kV (f) 21 kV

(g) 7 kV (h) 14 kV (i) 21 kV

Figure 4.8 SEM images (at a magnification of 500) of: (a-c) 10%; (d-f) 20%; (g-i) 30% (w/v) PS in EA system for effect of applied voltage by fixing the collection distance (i.e. 7 kV/7 cm, 14 kV/7 cm, and 21 kV/7 cm). Under positive polarity of the emitting electrode and the scale bar shown is for 50 μm.

Remark – means jet has not been found under this condition

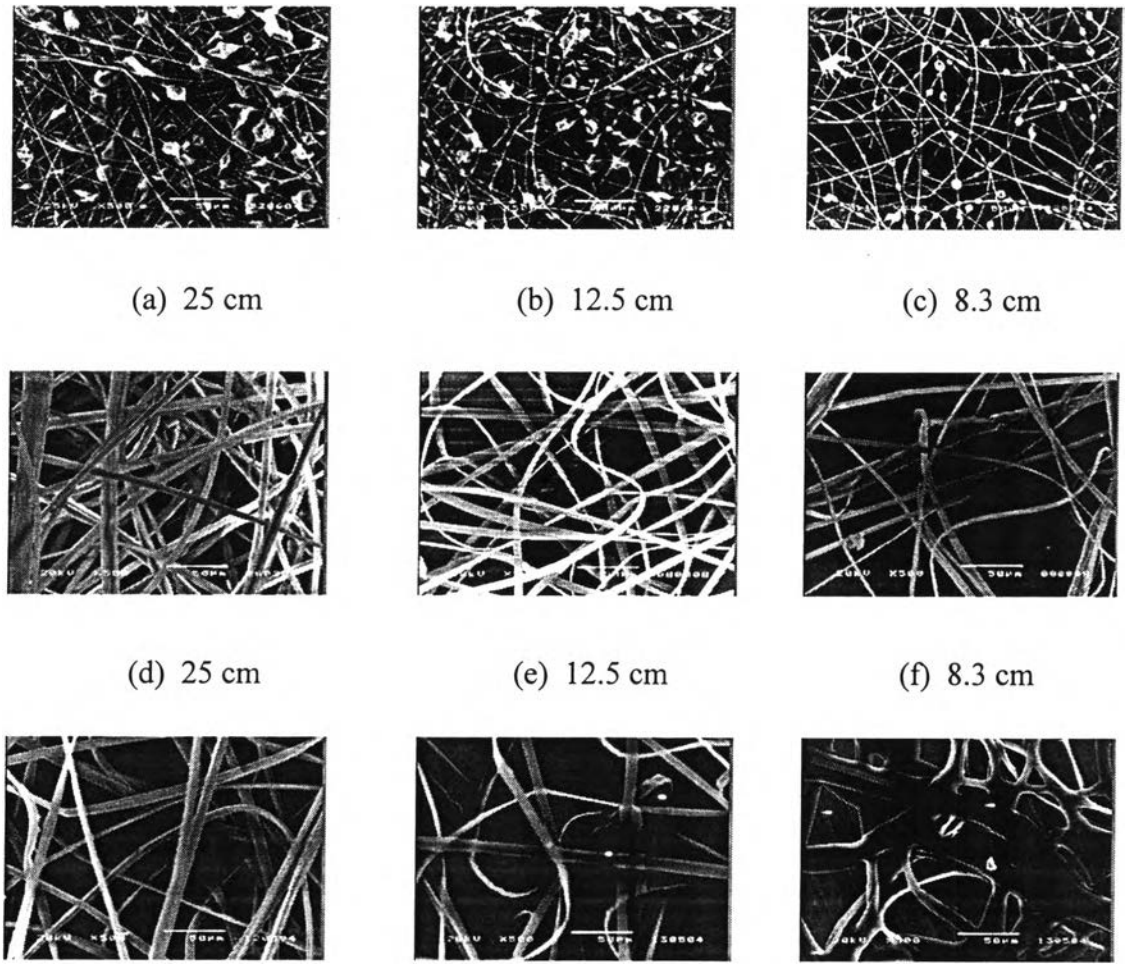

(a) 25 cm (b) 12.5 cm (c) 8.3 cm

(d) 25 cm (e) 12.5 cm (f) 8.3 cm

(g) 25 cm (h) 12.5 cm (i) 8.3 cm

Figure 4.9 SEM images (at a magnification of 500) of: (a-c) 10%; (d-f) 20%; (g-i) 30% (w/v) PS in MEK system for effect of collection distance by fixing the applied voltage (i.e. 25 kV/25 cm, 25 kV/12.5 cm, and 25 kV/8.3 cm). Under positive polarity of the emitting electrode and the scale bar shown is for 50 μm.

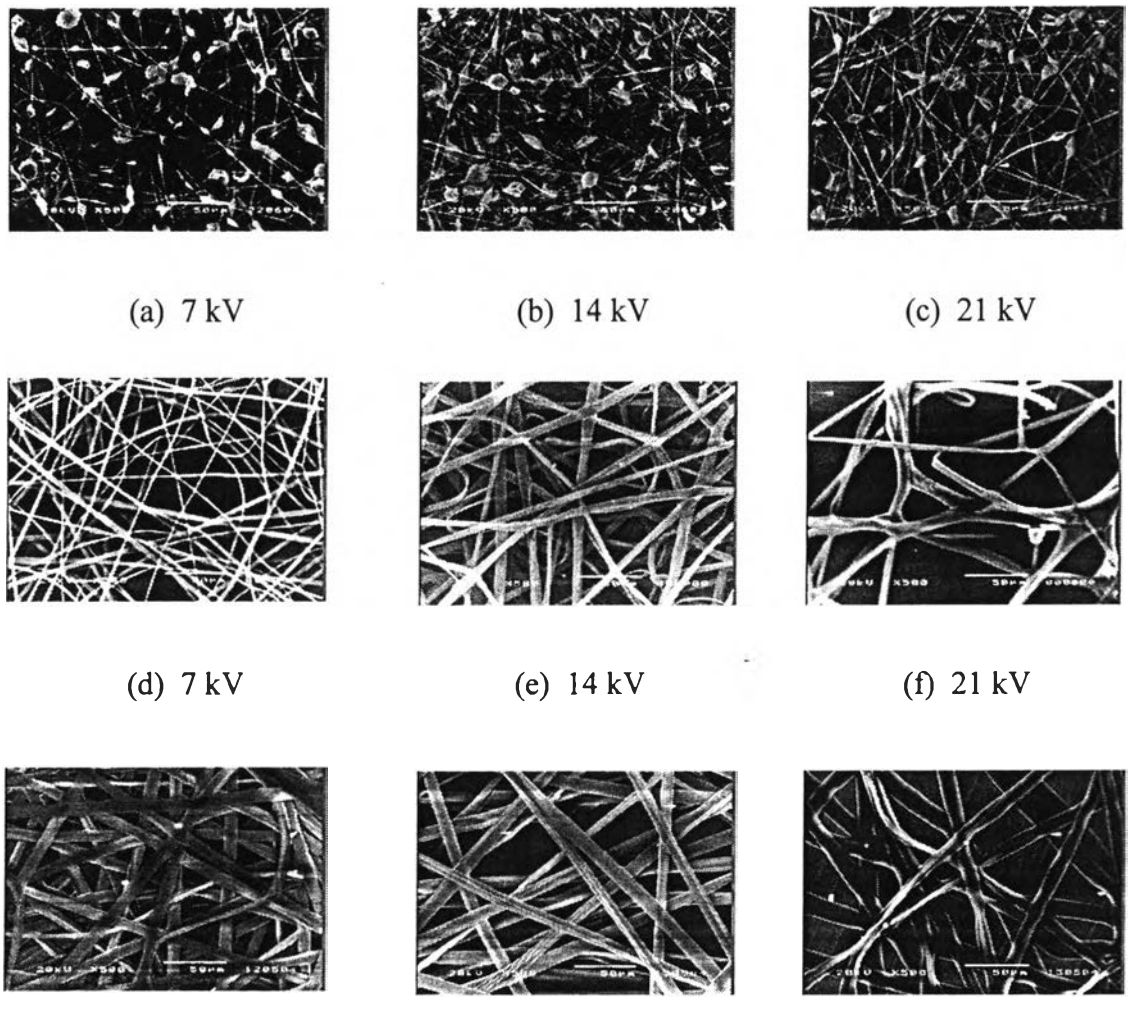

(a) 7 kV (b) 14 kV (c) 21 kV

(d) 7 kV (e) 14 kV (f) 21 kV

(g) 7 kV (h) 14 kV (i) 21 kV

Figure 4.10 SEM images (at a magnification of 500) of: (a-c) 10%; (d-f) 20%; (g-i) 30% (w/v) PS in MEK system for effect of applied voltage by fixing the collection distance (i.e. 7 kV/7 cm, 14 kV/7 cm, and 21 kV/7 cm). Under positive polarity of the emitting electrode and the scale bar shown is for 50 μm.

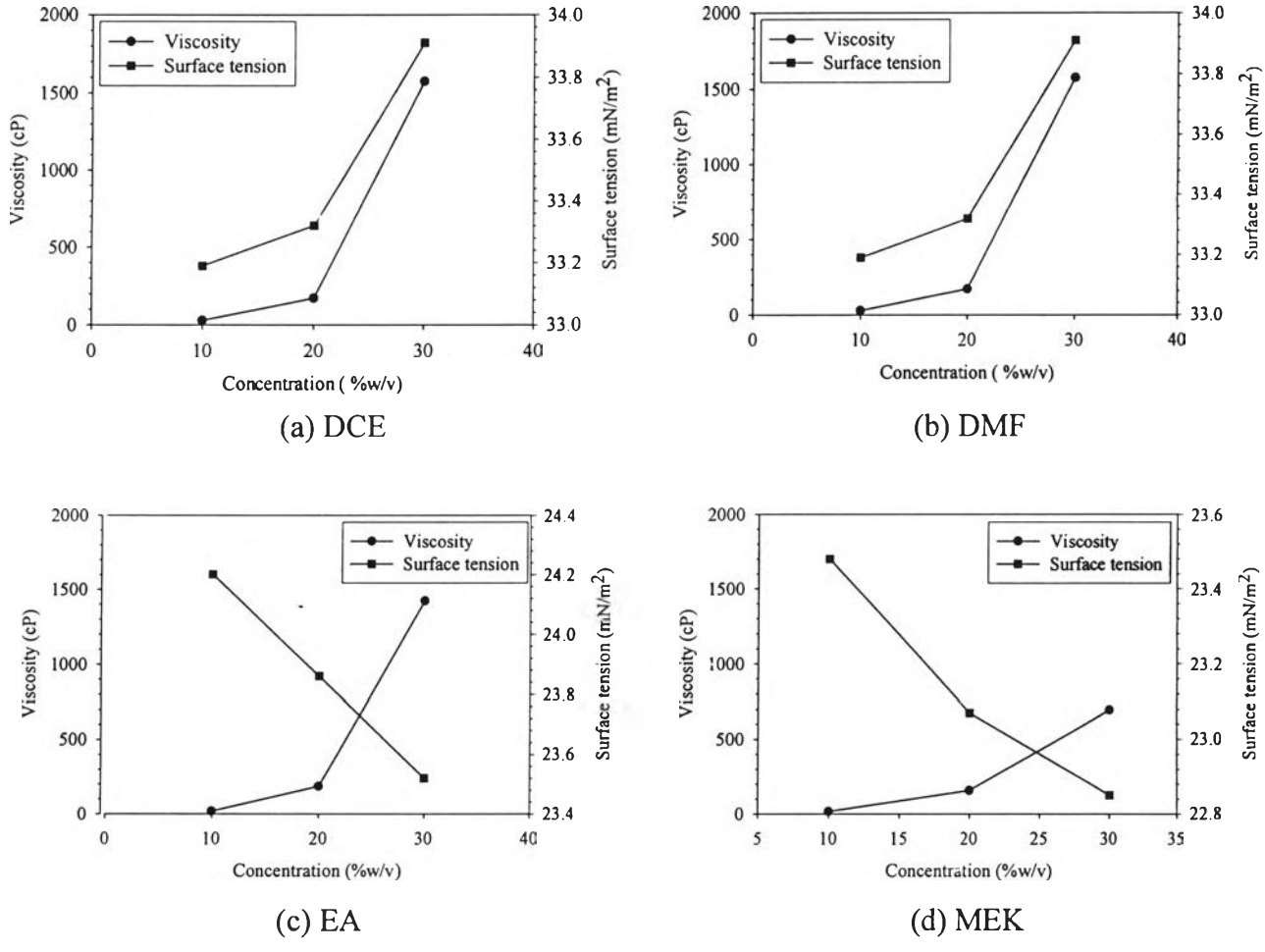

Figure 4.11 Plot of viscosity and surface tension for four type different solvents: (a) DCE; (b) DMF; (c) EA; and (d) MEK as a function of as-prepared PS concentration (%w/v).

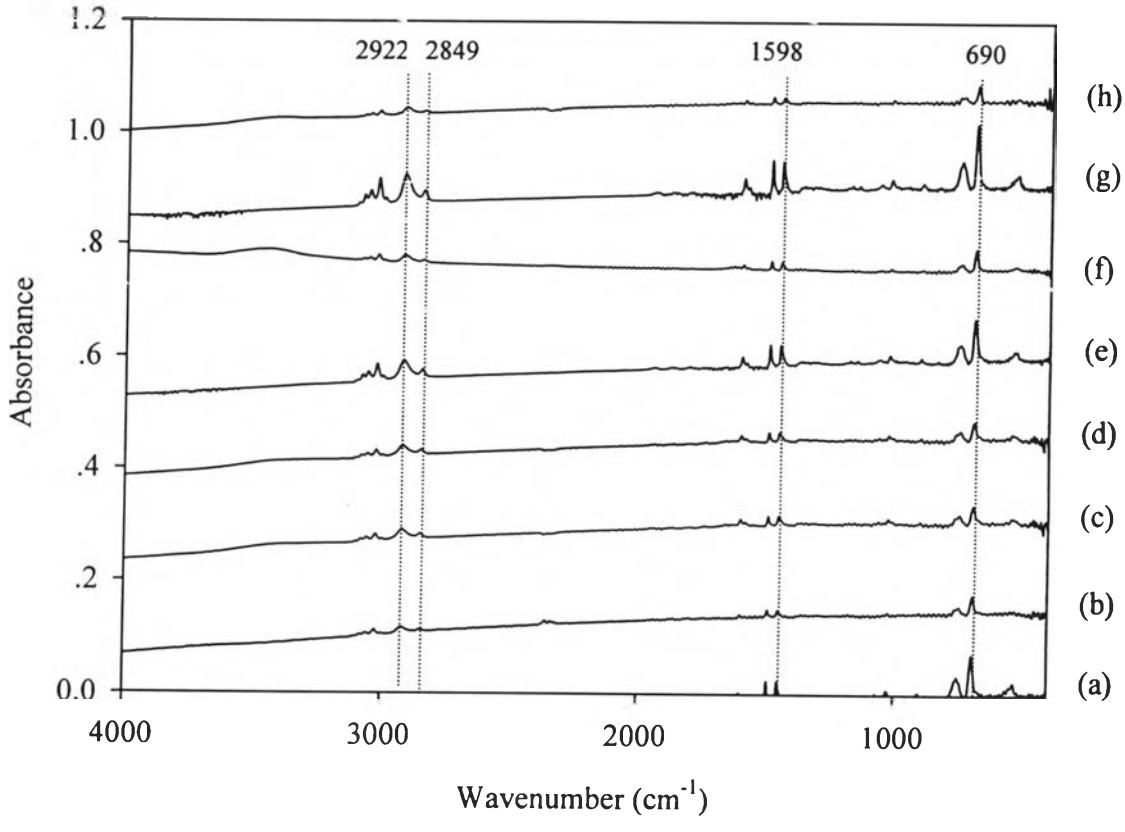

Figure 4.12 IR spectra of as-spun PS fibers from solution of: (a) 10%(w/v) PS in DCE; (b) 30%(w/v) PS in DCE; (c) 10%(w/v) PS in DMF; (d) 30%(w/v) PS in DMF; (e) 10%(w/v) PS in EA; (f) 30%(w/v) PS in EA; (g) 10%(w/v) PS in MEK; and (h) 30%(w/v) PS in MEK. Applied electrical filed strength was 25 kV/8.3 cm.

Table 4.5 Analysis of IR spectra of as-spun polystyrene fiber

Peaks observed in as-spun PS fibers (cm^{-1})	Assignment
690	–C-H bending of aromatic
1598	C=C stretching of aromatic ring
2849	aliphatic C-H stretching
2922	=C-H stretching of aromatic

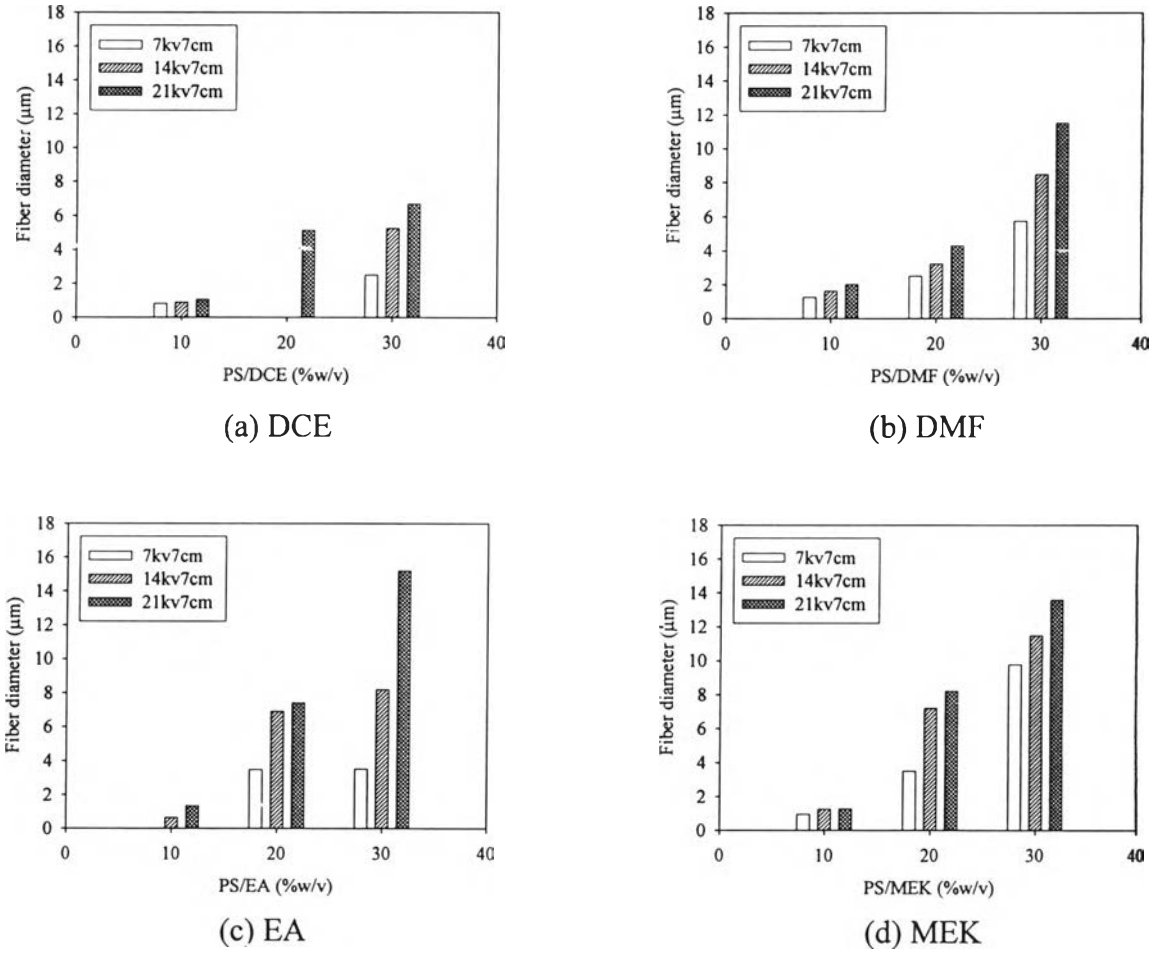

Figure 4.13 Effect of applied voltage by fixing the collection distance (i.e. 7 kV/7 cm, 14 kV/7 cm, and 21 kV/7 cm) on the fiber diameter of PS at 10%, 20%, and 30% (w/v) in four type different solvents. Under positive polarity of the emitting electrode.

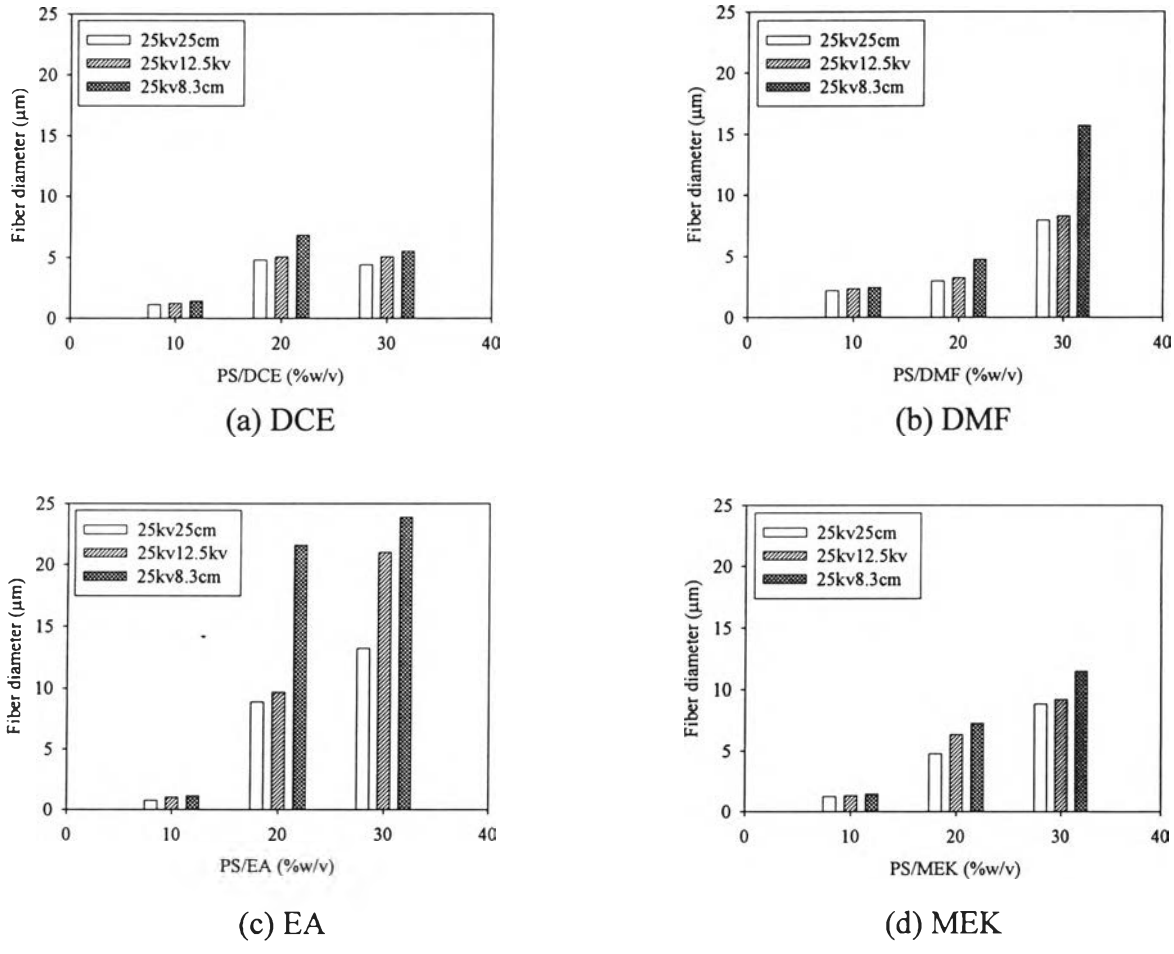

Figure 4.14 Effect of collection distance by fixing the applied voltage (i.e. 25 kV/25 cm, 25 kV/12.5 cm, and 25 kV/8.3 cm) on the fiber diameter of PS at 10%, 20%, and 30% (w/v) in four type different solvents. Under positive polarity of the emitting electrode.

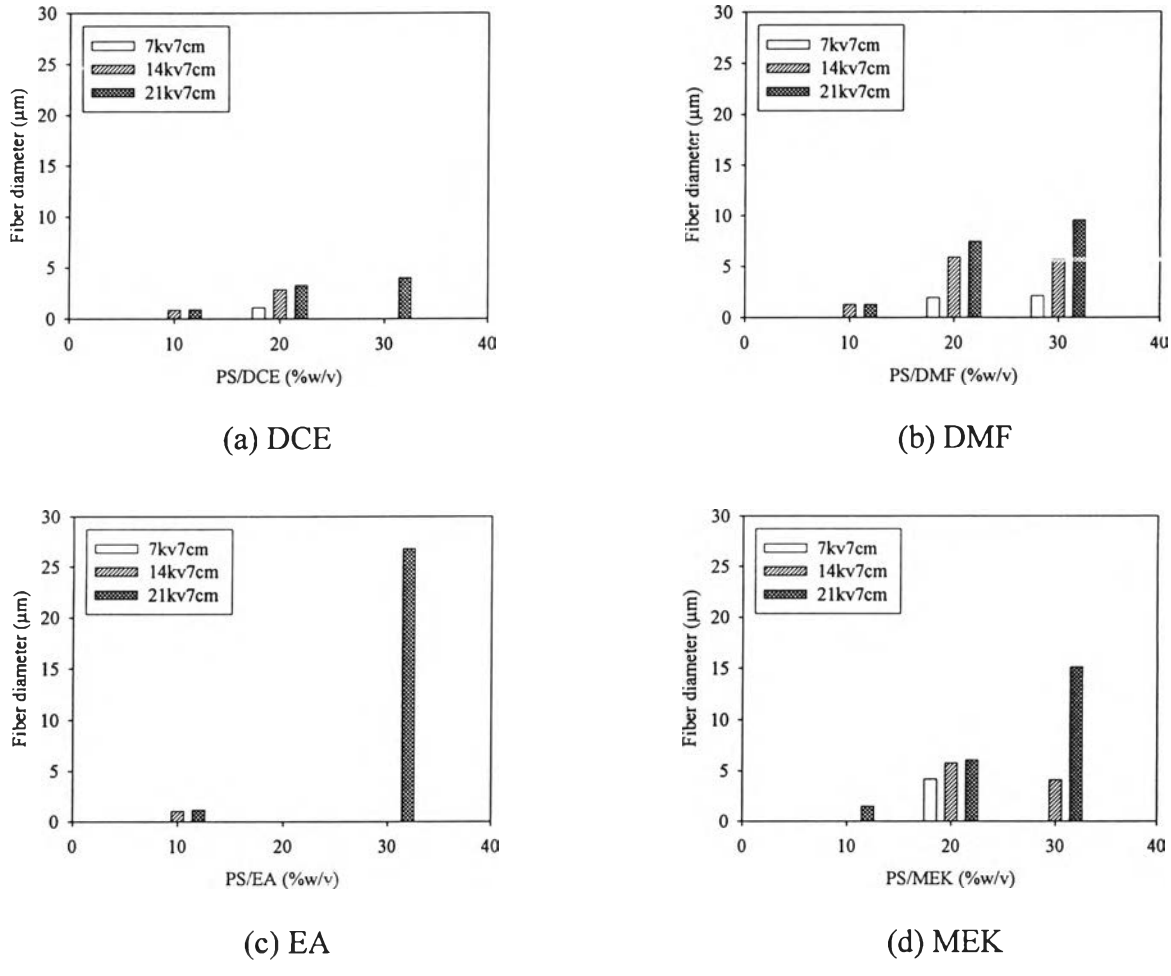

(a) DCE (b) DMF

(c) EA (d) MEK

Figure 4.15 Effect of applied voltage by fixing the collection distance (i.e. 7 kV/7 cm, 14 kV/7 cm, and 21 kV/7 cm) on the fiber diameter of PS at 10%, 20%, and 30% (w/v) in four type different solvents. Under negative polarity of the emitting electrode.

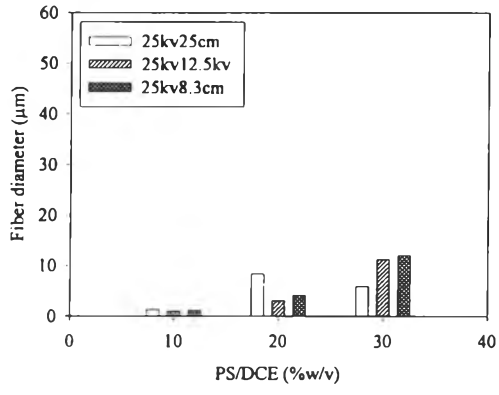

(a) DCE

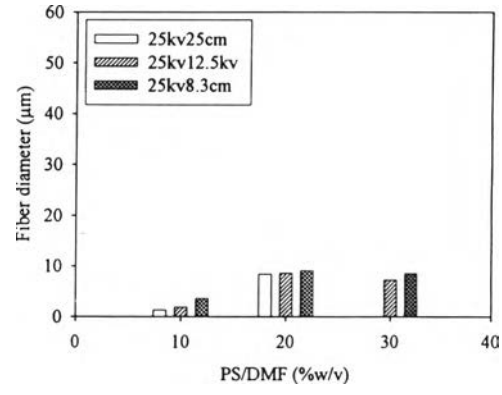

(b) DMF

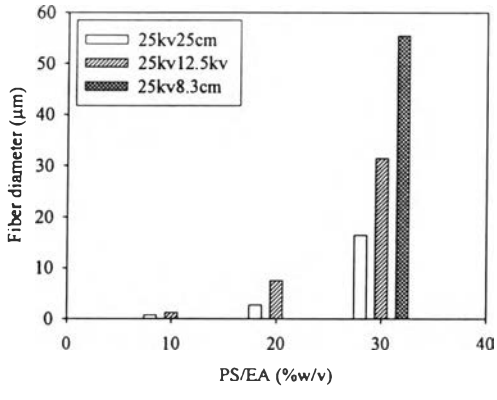

(c) EA

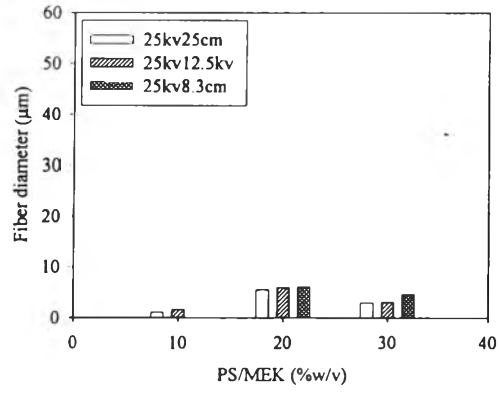

(d) MEK

Figure 4.16 Effect of collection distance by fixing the applied voltage (i.e. 25 kV/25 cm, 25 kV/12.5 cm, and 25 kV/8.3 cm) on the fiber diameter of PS at 10%, 20%, and 30% (w/v) in four type different solvents. Under negative polarity of the emitting electrode.

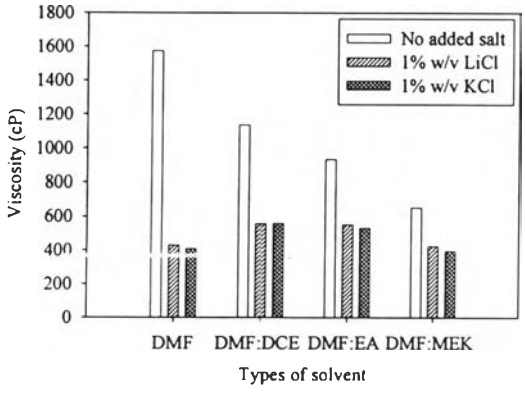

(a)

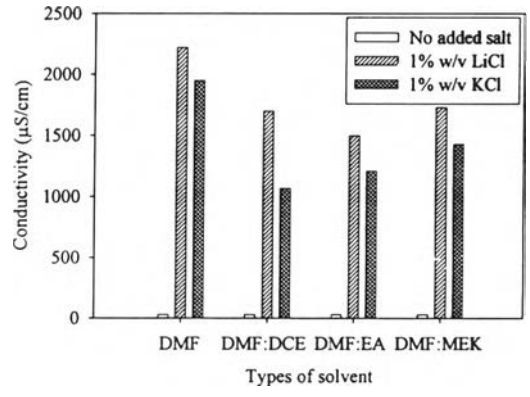

(b)

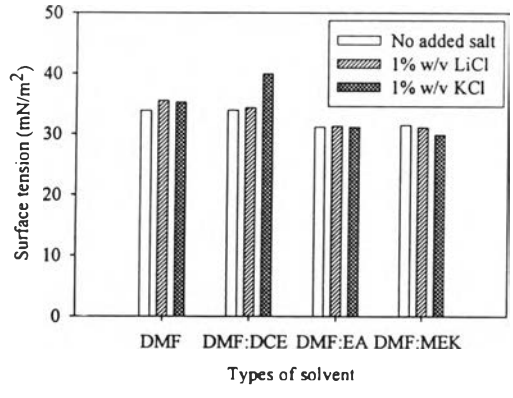

(c)

Figure 4.17 Effect of salt on: (a) viscosity; (b) conductivity; and (c) surface tension.

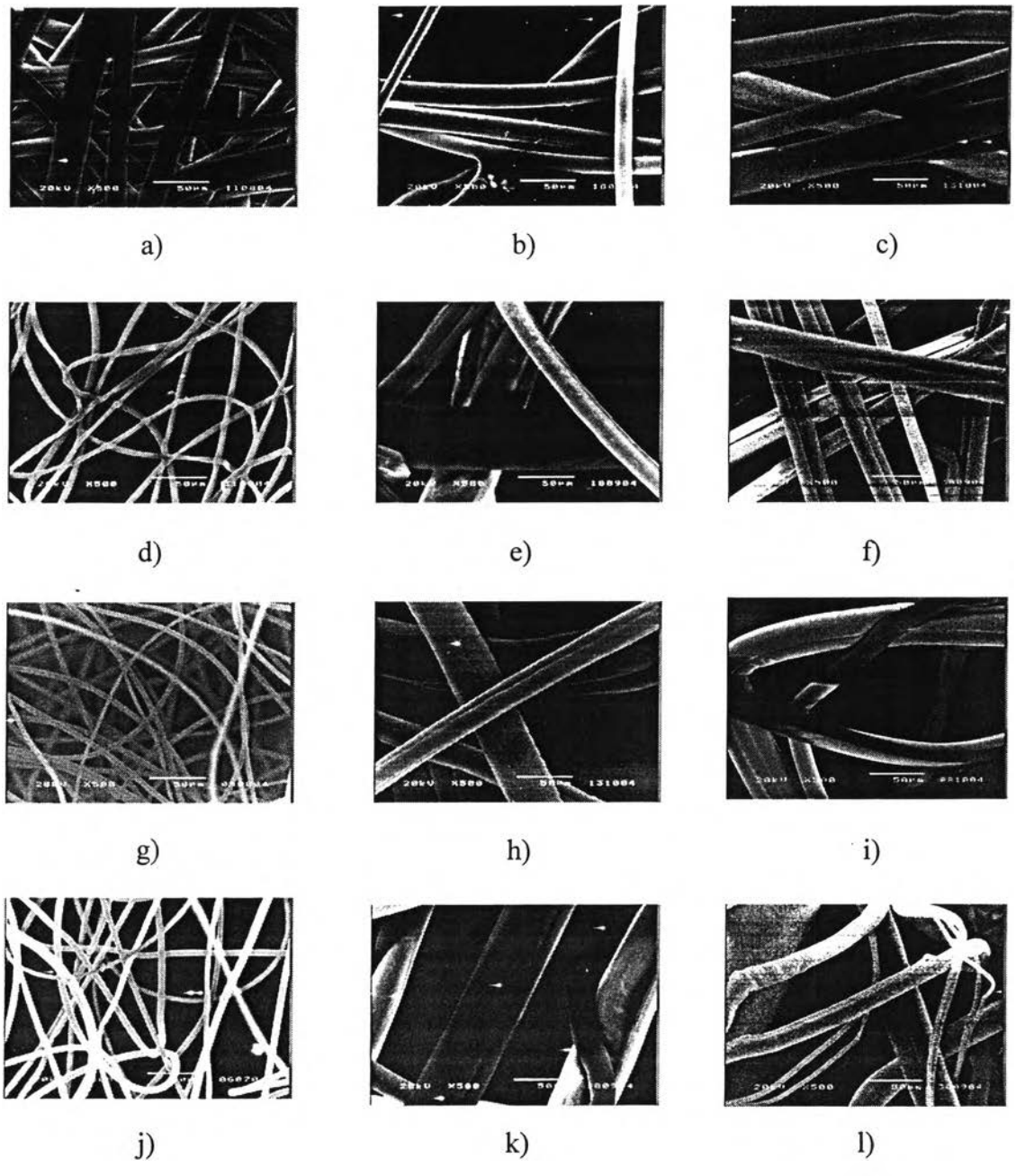

Figure 4.18 SEM images of as-spun fibers from: (a-c) 30% (w/v) PS/DMF; (d-f) 30% (w/v) PS/DMF:DCE(75/25); (g-i) 30% (w/v) PS/DMF:EA(75/25); (j-l) 30% (w/v) PS/DMF:MEK(75/25) with (b, e, h, k) 1% (w/v) of LiCl; (c, f, i, l) 1% w/v of KCl. Applied electrical field was 20kV/15 cm and the scale bar shown is for 50 μm.

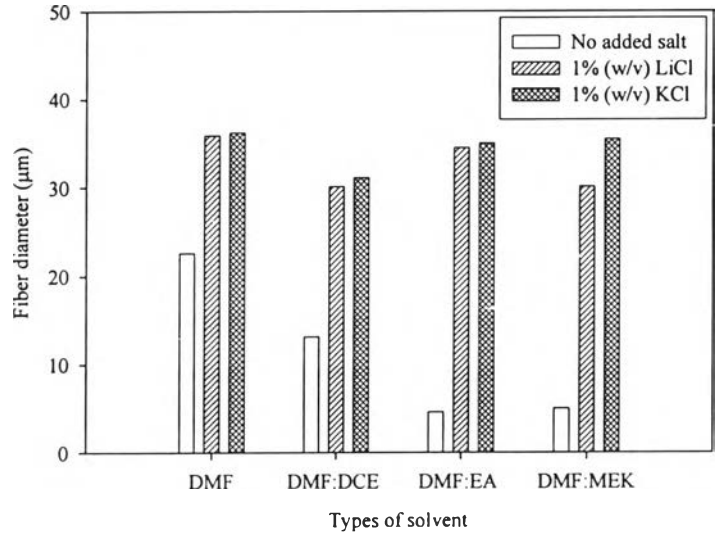

Figure 4.19 Fiber diameter of as-spun fibers from 30% (w/v) PS solution in various types of solvent with added 1% (w/v) salt. Applied electrical field was 21 kV/7 cm.

Table 4.6 Solution properties of mixed solvent systems between DMF and various solvents

Solution system	viscosity (cP)			conductivity (μS/cm)			surface tension (mN/m^2)		
(% v/v)	10%	20%	30%	10%	20%	30%	10%	20%	30%
DMF:DCE									
75/25	28.4	202	1136	25.50	16.36	1.55	34.22	33.96	33.95
50/50	31.8	225	867	27.80	17.40	1.60	33.74	33.83	34.60
25/75	34.6	214	813	15.43	12.50	0.97	32.80	33.35	33.92
DMF:EA									
75/25	23.6	181	933	1.58	1.10	0.60	31.56	31.27	31.16
50/50	20.8	175	818	1.09	0.80	0.49	28.33	28.07	27.89
25/75	18.4	158	580	0.47	0.40	0.27	25.37	25.32	26.16
DMF:MEK									
75/25	90.6	178	652	1.68	2.03	0.60	32.00	31.79	31.48
50/50	85.8	162	637	2.95	3.57	0.55	28.54	27.63	27.44
25/75	75.6	144	523	3.05	0.57	0.51	26.34	25.75	25.26

(a) DMF:DCE = 100/0

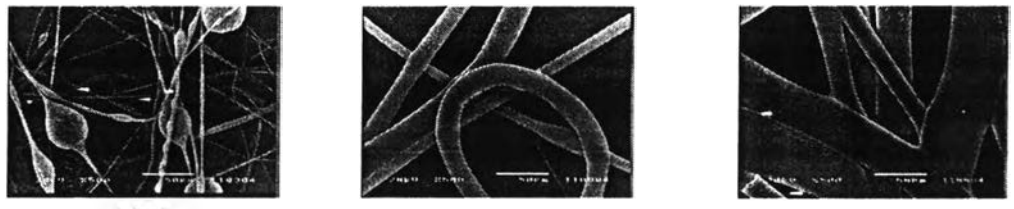

10% 20% 30%

(b) DMF:DCE = 75/25

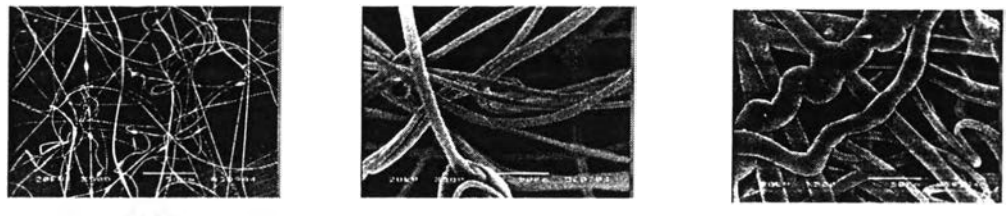

10% 20% 30%

(c) DMF:DCE = 50/50

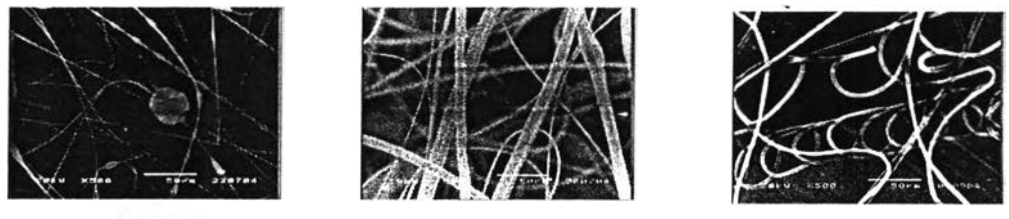

10% 20% 30%

(d) DMF:DCE = 25/75

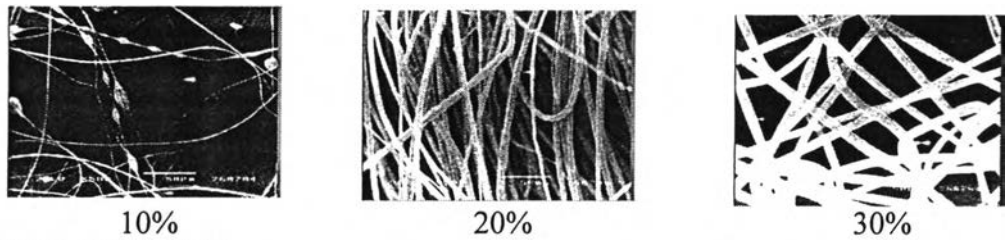

10% 20% 30%

(e) DMF:DCE = 0/100

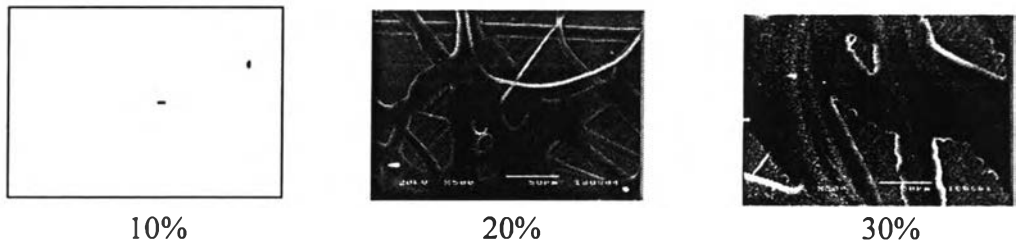

10% 20% 30%

Figure 4.20 SEM images of as-spun fibers obtained from PS solutions at 10%, 20%, and 30% (w/v) in a mixed solvent of DMF and DCE in various volumetric ratios: a) 100/0; b) 75/25; c) 50/50; d) 25/75; and e) 0/100. Applied electrical field was 20 kV/10 cm and the scale bar shown is for 50 μm.

Remark – means jet has not been found under this condition

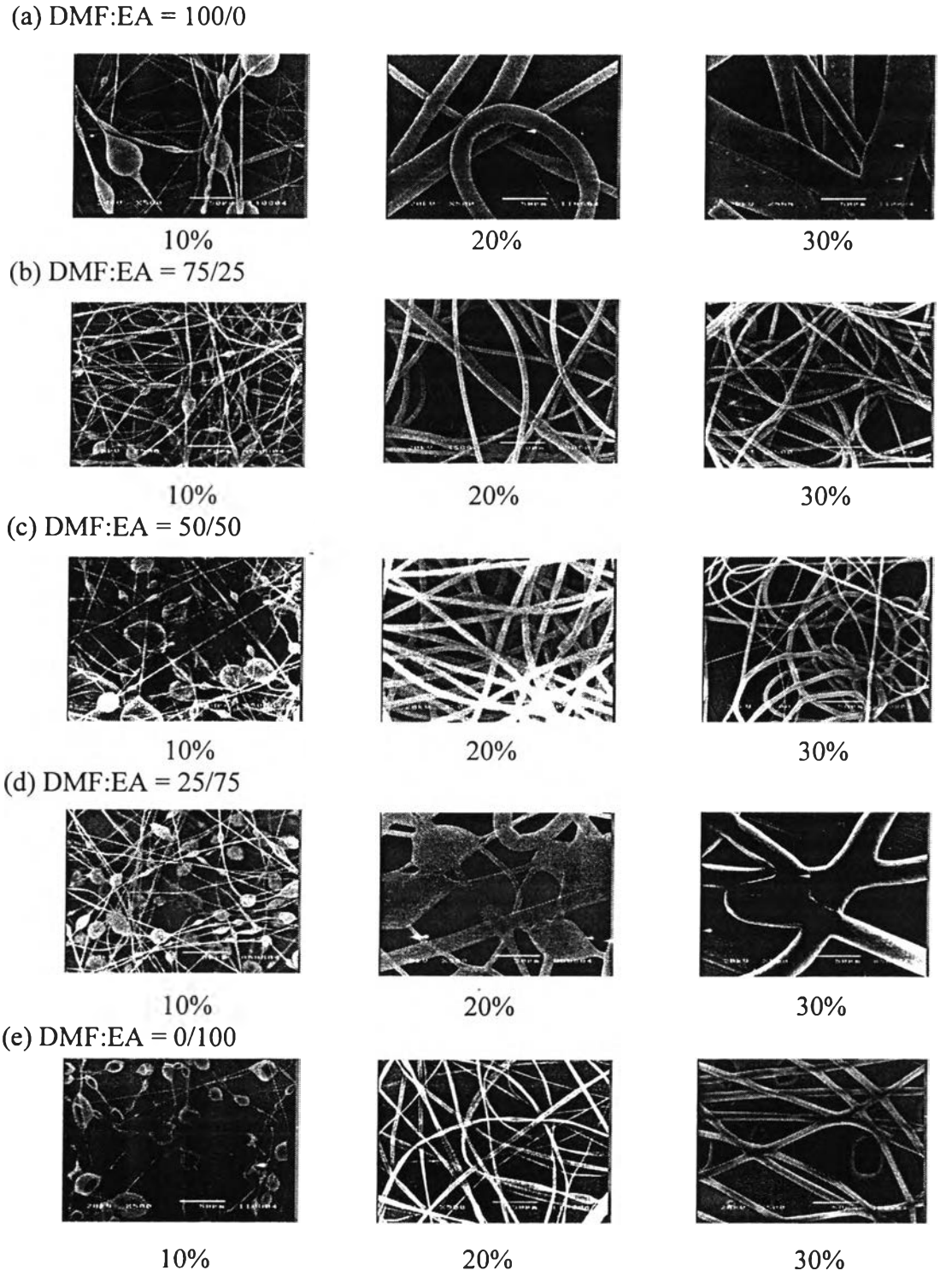

Figure 4.21 SEM images of as-spun fibers obtained from PS solutions at 10%, 20%, and 30% (w/v) in a mixed solvent of DMF and EA in various volumetric ratios: a) 100/0; b) 75/25; c) 50/50; d) 25/75; and e) 0/100. Applied electrical field was 20 kV/10 cm and the scale bar shown is for 50 μm.

(a) DMF:MEK = 100/0

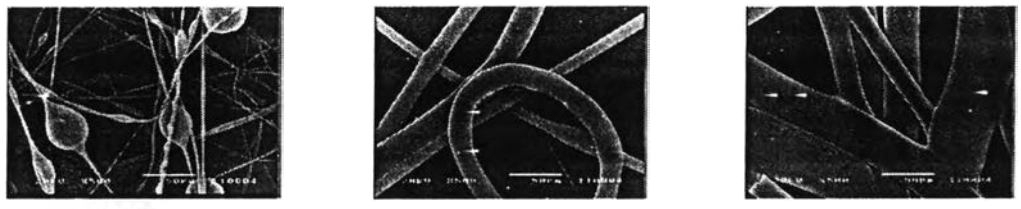

10% 20% 30%

(b) DMF:MEK = 75/25

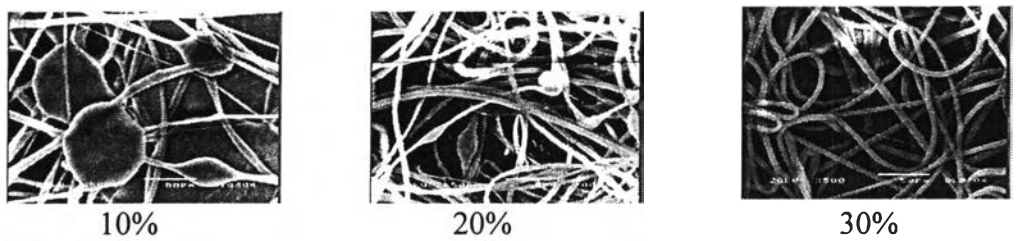

10% 20% 30%

(c) DMF:MEK = 50/50

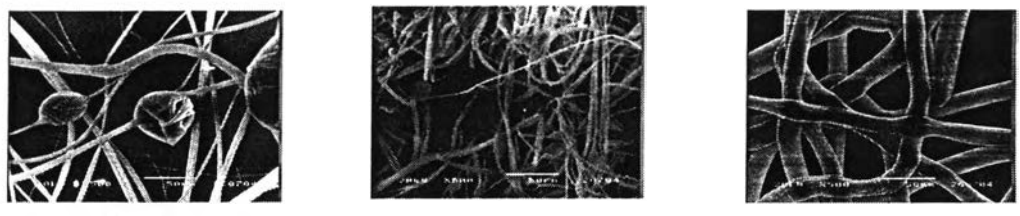

10% 20% 30%

(d) DMF:MEK = 25/75

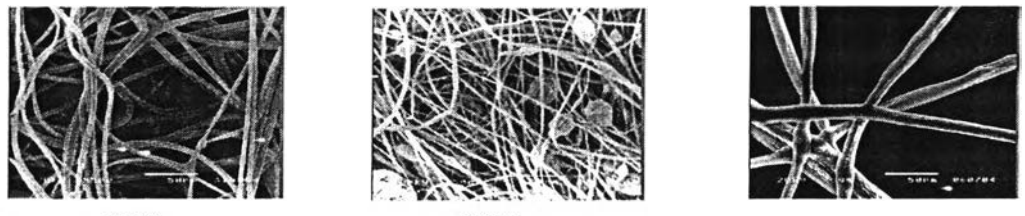

10% 20% 30%

(e) DMF:MEK = 0/100

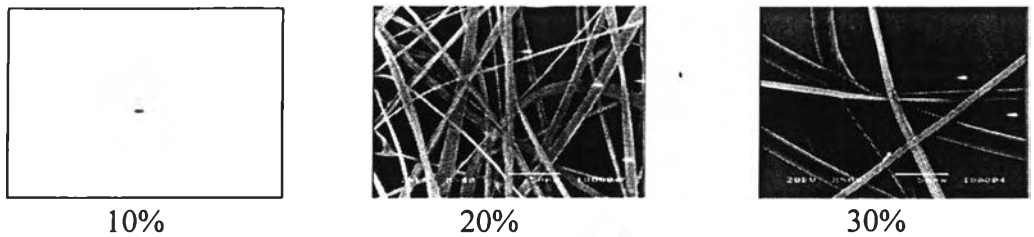

10% 20% 30%

Figure 4.22 SEM images of as-spun fibers obtained from PS solutions at 10%, 20%, and 30% (w/v) in a mixed solvent of DMF and MEK in various volumetric ratios a) 100/0; b) 75/25; c) 50/50; d) 25/75; and e) 0/100. Applied electrical field was 20 kV/10 cm and the scale bar shown is for 50 μm.

Remark – means jet has not been found under this condition